



HAL
open science

The absence of VGLUT3 predisposes to cocaine abuse by increasing dopamine and glutamate signaling in the nucleus accumbens

D Sakae, F. Marti, S Lecca, F. Vorspan, E Martín-García, L. Morel, A Henrion, J. Gutierrez-Cuesta, A. Besnard, N Heck, et al.

► To cite this version:

D Sakae, F. Marti, S Lecca, F. Vorspan, E Martín-García, et al.. The absence of VGLUT3 predisposes to cocaine abuse by increasing dopamine and glutamate signaling in the nucleus accumbens. *Molecular Psychiatry*, 2015, 20 (11), pp.1448-1459. 10.1038/mp.2015.104 . hal-02372449

HAL Id: hal-02372449

<https://hal.science/hal-02372449>

Submitted on 8 Apr 2024

HAL is a multi-disciplinary open access archive for the deposit and dissemination of scientific research documents, whether they are published or not. The documents may come from teaching and research institutions in France or abroad, or from public or private research centers.

L'archive ouverte pluridisciplinaire **HAL**, est destinée au dépôt et à la diffusion de documents scientifiques de niveau recherche, publiés ou non, émanant des établissements d'enseignement et de recherche français ou étrangers, des laboratoires publics ou privés.

The absence of VGLUT3 predisposes to cocaine abuse by increasing dopamine and glutamate signaling in the nucleus accumbens

Diana Yae Sakae^{1,2,3,4,†}, Fabio Marti^{1,2,3,4,†}, Salvatore Lecca^{1,5,6,†}, Florence Vorspan^{7,8,9,10}, Elena Martín-García¹¹, Lydie Jacqueline Morel^{1,2,3,4}, Annabelle Henrion^{7,10,12,13}, Javier Gutiérrez-Cuesta¹¹, Antoine Besnard^{1,2,3}, Nicolas Heck^{1,2,3}, Etienne Herzog^{1,2,3}, Susanne Bolte¹⁴, Vania F. Prado¹⁵, Marco A.M. Prado¹⁵, Frank Bellivier^{7,8,9,10}, Chin B. Eap^{16,17}, Séverine Crettol¹⁶, Peter Vanhoutte^{1,2,3}, Jocelyne Caboche^{1,2,3}, Alain Gratton⁴, Luc Moquin⁴, Bruno Giros^{1,2,3,4,7}, Rafael Maldonado¹¹, Stéphanie Daumas^{1,2,3}, Manuel Mameli^{1,5,6}, Stéphane Jamain^{7,10,12,13,*}, Salah El Mestikawy^{1,2,3,4,7,*}

¹Sorbonne Universités, Université Pierre et Marie Curie (UPMC) Paris 06, Institut de Biologie Paris-Seine (IBPS), UMR119 Neurosciences Paris Seine, F-75005, Paris, France.

²Institut National de la Santé et de la Recherche Médicale (INSERM), UMR-S 1130, Neurosciences Paris Seine, F-75005, Paris, France.

³Centre National de la Recherche Scientifique (CNRS) UMR 8246, Neurosciences Paris Seine, F-75005, Paris, France.

⁴Douglas Hospital Research Center, Department of Psychiatry, McGill University, 6875 boulevard Lasalle Verdun, QC, Canada.

⁵Institut du Fer à Moulin, 17 rue du Fer à Moulin, 75005 Paris, France.

⁶Institut National de la Santé et de la Recherche Médicale (INSERM), UMR-S 839, 17 rue du Fer à Moulin, 75005 Paris, France.

⁷Fondation FondaMental, Créteil, France.

⁸Institut National de la Santé et de la Recherche Médicale (INSERM), U705, Centre National de la Recherche Scientifique (CNRS) UMR 8206, Université Paris Descartes, Université Denis Diderot, PRES Sorbonne Paris Cité, Paris, France.

⁹Assistance Publique-Hôpitaux de Paris, GH Saint-Louis - Lariboisière - F. Widal, Service de Psychiatrie, Paris, France.

¹⁰Institut National de la Santé et de la Recherche Médicale (INSERM), Psychiatrie Translationnelle, U955, Créteil, 94000, France.

¹¹Departament de Ciències Experimentals i de la Salut, Universitat Pompeu Fabra, PRBB, C/ Dr. Aiguader 88, 08003, Barcelona, Spain.

¹²Université Paris Est, Faculté de Médecine, Créteil, 94000, France.

¹³Assistance Publique-Hôpitaux de Paris, Hôpital H. Mondor – A. Chenevier, Pôle de Psychiatrie, Créteil, 94000, France.

¹⁴Cellular Imaging Facility, Institut de Biologie Paris-Seine (IBPS), Sorbonne Universités, Université Pierre et Marie Curie (UPMC), F-75005, Paris, France.

¹⁵Robarts Research Institute, Department of Anatomy & Cell Biology and Department of Physiology and Pharmacology, The University of Western Ontario, London, Ontario, N6A 5K8, Canada.

¹⁶Unit of Pharmacogenetics and Clinical Psychopharmacology, Centre for Psychiatric Neuroscience, Department of Psychiatry, Lausanne University Hospital, Hospital of Cery, Prilly, Switzerland.

¹⁷School of Pharmacy, Department of Pharmaceutical Sciences, University of Geneva, University of Lausanne, Geneva, Switzerland.

*Correspondence to: SEM (salah.elmestikawy@mcgill.ca) and SJ (stephane.jamain@inserm.fr).

†These authors contributed equally to this work.

Short Title: VGLUT3 in the nucleus accumbens and cocaine abuse

Keywords: addiction; nucleus accumbens; cholinergic interneurons (TANs); co-transmission; acetylcholine; glutamate; vesicular acetylcholine transporter (VAChT); vesicular glutamate transporter type 3 (VGLUT3).

Author Contributions:

D.Y.S., L.J.M., E.M.G. and J.G-C. performed the behavioral experiments with the help of S.D.

F.M. performed the *in vivo* electrophysiology and voltammetry with the help of D.Y.S, G.M. and A.G.

D.Y.S. and L.J.M. performed the anatomical experiments with the help of S.B. and E.H.

D.Y.S., L.J.M. and A.B. performed the biochemical measurements with the help of N.H., P.V.H. and J.C.

M.M. and S.L. performed the *in vitro* electrophysiology experiments.

The genetic studies were designed by S.J. and performed by S.J. with the help of F.V., A.H. and F.B.

C.B.E., S.C.W., F.V. and F.B. recruited subjects with severe addiction and unaffected controls.

V.P. and M.P. generated the VACHT mutant mice and helped with the manuscript.

S.E.M. designed the study and wrote the manuscript with the help of D.Y.S., F.M., R.M., B.G., M.M. and S.J.

Abstract

Tonically active cholinergic interneurons (TANs) from the nucleus accumbens (NAc) are centrally involved in reward behavior. TANs express a vesicular glutamate transporter referred to as VGLUT3 and thus use both acetylcholine (ACh) and glutamate as neurotransmitters. The respective roles of each transmitter in the regulation of reward and addiction are still unknown. In this study, we showed that disruption of the gene that encodes VGLUT3 (*Slc17a8*) markedly increased cocaine self-administration in mice. Concomitantly, the amount of dopamine (DA) release was strongly augmented in the NAc of VGLUT3^{-/-} mice due to a lack of signaling by metabotropic glutamate receptors (mGLURs). Furthermore, dendritic spines and glutamatergic synaptic transmission on medium spiny neurons were increased in the NAc of VGLUT3^{-/-} mice. Increased DA and glutamate signaling in the NAc are hallmarks of addiction. Our study shows that TANs use glutamate to reduce DA release and decrease reinforcing properties of cocaine in mice. Interestingly, we also observed an increased frequency of rare variations in *SLC17A8* in a cohort of severe drug abusers compared to controls. Our findings identify VGLUT3 as an unexpected regulator of drug abuse.

INTRODUCTION

Drug addiction is a compulsive pattern of drug-taking/drug-seeking behavior with major adverse repercussions. Although the molecular mechanisms underlying addiction are not completely understood, all addictive substances regulate the reward circuit by increasing dopamine (DA) release in the nucleus accumbens (NAc).¹⁻³ GABAergic medium spiny neurons (MSNs) are the major input target as well as the output of the NAc. MSNs are dynamically regulated by dopaminergic fibers that originate from the ventral tegmental area (VTA) and by local interneurons, such as the tonically active cholinergic interneurons (TANs). Fine-tuning the balance between DA and acetylcholine (ACh) is key for the correct processing of reward-directed behaviors. However, the precise role of TANs and ACh in the NAc is not well understood. VGLUT3 expression in TANs was recently found to increase ACh vesicular accumulation and release⁴ and to confer on TANs the ability to signal with glutamate as well as with ACh.⁵ Surprisingly, mice without the ability to secrete ACh experience minimal alterations in their behavioral responses to cocaine.⁶ Interestingly, silencing VGLUT3 in mice results in marked cocaine-induced locomotor activity⁴, suggesting that glutamate released by TANs is instrumental in regulating reinforced responses to cocaine.

In this study, we analyzed the implications of VGLUT3 in reward and addiction. We found that the hedonic effects of cocaine were exacerbated in VGLUT3^{-/-} mice. We also showed that TANs from the NAc used both glutamate and ACh to decrease or increase DA release, respectively. Finally, we reported a higher rate of non-synonymous mutations in the gene encoding VGLUT3 in patients with severe addictions compared to controls. Our results suggest that TANs and VGLUT3 in the NAc act as protective filters against the reinforcing properties of substances of abuse such as cocaine.

MATERIALS AND METHODS

Human populations

A total of 230 adult subjects with cocaine and/or opiate dependence from two different studies, METHADOSE (n=144) and PSYCHOCOKE (n=86), were included. Written informed consent was obtained from all participants. Institutional review board approval was obtained (Saint-Louis Hospital Ethic Committee, Paris, December 22, 2008).

For inclusion in the METHADOSE study, patients had to be methadone-maintained opiate-dependent with a stable methadone regimen for at least 3 months.

For inclusion in the PSYCHOCOKE study, patients had to be current cocaine users. Only cocaine-dependent patients were considered in the present genetic analysis.

Patients were primarily males (75%) with a mean age at interview of 40.5 ± 9.4 years. Most of them were Caucasian (88%), 9% were of sub-Saharan African origin and 3% were of Asian origin. All were 100% dependent with a mean duration of illness of 16 ± 10 years; 15% were cocaine-dependent only, 25% were opiate-dependent only and 60% were dependent on both cocaine and opiates. In addition, 55% of patients had a positive lifetime history of alcohol-dependence, 43% had a lifetime history of benzodiazepine dependence and 64% had a lifetime history of cannabis dependence.

Additionally, 213 unaffected controls of French origin were recruited from among blood donors attending the Henri Mondor Hospital (Créteil, France). The unaffected controls were assessed using the Diagnostic Interview for Genetic Studies (DIGS), and their family history of psychiatric disorders was determined with the Family Interview for Genetic Studies (FIGS). Only subjects with neither a personal nor a family history of affective disorders, severe addiction or suicide attempts were included. DNA from 390 controls of African origin (69 from Tunisia, 119 from Morocco, 75 from Algeria and 127 from sub-Saharan Africa) were generously provided by Dr.

Ryad Tamouza (Hôpital Saint Louis, Paris, France) and used to examine the allele frequency of rs45610843.

DNA from 265 patients with opiate dependence in methadone maintenance treatment have been used for the replication cohort. These subjects were included in a multi-center study in Switzerland as previously described in detail elsewhere ⁷ and a proportion of the patients was also cocaine abusers.

All subjects signed a written informed consent, and local institutional review boards approved this protocol.

***SLC17A8* sequence analysis**

For each individual, genomic DNA was isolated from blood leukocytes using a standard procedure. The *SLC17A8* coding regions were amplified before sequencing using the BigDye® Terminator v3.1 Cycle Sequencing Kit (Life Technologies, Carlsbad, CA, U.S.A.) and run on a 16-Capillary ABI PRISM® 3130xl genetic analyzer. All primers used for the PCR amplifications and sequence analyses are available on request. Genotyping of 390 additional controls of African origin was performed to examine the allele frequency of rs45610843.

Animals

Animal studies were performed in accordance with the European Communities Council Directive (86/809/EEC) regarding the care and use of animals for experimental procedures in compliance with the *Ministère de l'Agriculture et de la Forêt, Service Vétérinaire de la Santé et de la Protection Animale* (permission # A 94-028-21).

The VGLUT3^{-/-} mouse line has previously been described⁴ and was backcrossed on a

C57BL/6N background for ten generations. DRD1a-EGFP heterozygous mice (C57BL/6 background, Gensat) were crossed with VGLUT3^{-/-} to allow the direct assessment of fluorescent MSN. All experiments were carried out with wild type (WT), WT:DRD1a-EGFP VGLUT3^{-/-} and VGLUT3^{-/-}:DRD1a-EGFP 2-4-month-old male littermates, except for electrophysiological recordings that were performed with 30-40-day-old animals.

Animals were randomly allocated to experimental groups. Whenever possible, investigator was blinded during experimental procedures. Animals were excluded from the experimental data if and only they were detected by outlier test (Grubb's test – GraphPad Prism).

Drugs

Cocaine hydrochloride (Sigma-Aldrich, Saint-Louis, MO) was dissolved in a saline solution (0.9% NaCl w/v), except for the *in vivo* electrophysiological studies in which it was dissolved in water. Quinpirole hydrochloride and eticlopride hydrochloride (Tocris Bioscience, Bristol, UK) were dissolved in water. The mGLUR broad-spectrum antagonist LY341495 (Sigma-Aldrich) was dissolved in ACSF. Ketamine, xylazine, bicuculline and tetrodotoxin (Abcam, Cambridge, UK and Tocris, Bristol, UK) were dissolved in water, except for tetrodotoxin (1% citric acid).

Cocaine-induced locomotor activity and sensitization

Locomotor activity was measured in a cyclotron, which consisted of a circular corridor with four infrared beams placed at 90° angles (Imetronic, Pessac, France). Activity was counted as the consecutive interruption of two adjacent infrared beams (1/4 of a tour). To assess acute cocaine-induced locomotion, the animals (WT n=8; VGLUT3^{-/-} n=7) were placed in the cyclotron for 30 min for habituation and then injected with cocaine (10 mg/kg, *i.p.*). Locomotion was recorded for 60 min following the cocaine injection.

For the cocaine sensitization experiments, mice (WT n=6; VGLUT3^{-/-} n=6) were injected with saline and placed in the cyclotron for 60 min over 3 consecutive days for habituation. Starting on day 4, the mice were split into two groups: one group was treated with saline and the other with cocaine (10 mg/kg, *i.p.*, every day) for 5 consecutive days. This repeated exposure was followed by 5 days of withdrawal and by a cocaine challenge injection (10 mg/kg) on day 13. Locomotor activity was recorded 60 min after the saline or cocaine injection. Animals that underwent the cocaine sensitization protocol were used for spine labeling.

Cocaine conditioned place preference (CPP)

CPP was assessed using a Y-shaped apparatus (Imetronic, Pessac, France) as previously described.⁸ Two chambers were distinguished by different patterns on the floors and walls and were separated by a central neutral area. In the preconditioning phase, animals were allowed to explore both chambers for 18 min. In the conditioning phase, mice were randomly treated three times (three pairings) with saline (WT n=8; VGLUT3^{-/-} n=7), cocaine 2.5 mg/kg (WT n=10; VGLUT3^{-/-} n=11) or cocaine 5 mg/kg (WT n=7; VGLUT3^{-/-} n=7). Control animals received saline every day. After injections, they were confined to a given chamber for a period of 20 min. On the test day, the animals were again allowed to explore both chambers. Entries and time spent in each chamber were measured during both the pre- and post-conditioning phases. Data were expressed as the difference between the cocaine-paired minus the saline-paired chamber during pre- and post-conditioning.

Operant self-administration of cocaine

Cocaine self-administration experiments were performed as previously described.⁹⁻¹¹

Mice were anaesthetized with a ketamine/xylazine mixture (20 ml/kg, *i.p.*) and then implanted

with indwelling *i.v.* silastic catheters. Each 2-h daily self-administration session started with a priming injection of the drug. Cocaine was infused in 23.5 μ l over 2 s (0.5 mg/kg per injection, *i.v.*). Stimulation light (cue), located above the active hole, was paired with the delivery of the reinforcer. Mice (WT n=14; VGLUT3^{-/-} n=13) were trained under a fixed ratio 1 schedule of reinforcement (FR1; one nose-poke lead to the delivery of one dose of cocaine) over 5 consecutive daily sessions and under a fixed ratio 3 (FR3) over 5 consecutive daily sessions. The timeout period after infusion delivery was 15 s. Responses on the inactive hole and all responses elicited during the 15-s timeout period were also recorded. The criteria for self-administration behavior were achieved when all of the following conditions were met: 1) mice maintained stable, responding with less than 20% deviation from the mean of the total number of reinforcers earned in three consecutive sessions (80% of stability); 2) at least 75% of mice responding on the active hole; and 3) a minimum of 10 reinforcers per session. After the 10 FR sessions, animals were tested in a progressive ratio (PR) schedule of 3 h where the response requirement to earn the cocaine escalated according to the following series: 1-2-3-5-12-18-27-40-60-90-135-200-300-450-675-1,000. On day 12, mice were moved from the cocaine self-administration/training phase to the extinction phase. The experimental conditions during the extinction phase were similar to the cocaine self-administration sessions except that cocaine was not available, and light was not presented after nose-poking in the active hole. Mice were given 2-h daily sessions until they achieved the extinction criterion with a maximum of 18 sessions. The criterion for extinction was achieved when, during 3 consecutive sessions, mice completed a mean number of nose-pokes in the active hole consisting of less than 30% of the mean responses obtained during the three-day period to achieve the acquisition criteria for cocaine self-administration training. On day 28, all of the mice were tested under reinstatement induced by a cue during a 2-h session. The presentation of a conditioned environmental cue was performed to evaluate the reinstatement of cocaine-seeking behavior. The test for cue-induced

reinstatement was conducted under the same conditions used in the training phase except that cocaine was not available. The reinstatement criterion was achieved when nose-pokes in the active hole were double the number of nose-pokes in the active hole during the three consecutive days when the mice acquired the extinction criteria.

***In vivo* voltammetry**

Mice (WT n=14; VGLUT3^{-/-} n=16) were anesthetized with chloral hydrate (400 mg/kg, *i.p.*), and voltammetric electrodes (Aldrich, Milwaukee, WI) were implanted into the NAc (stereotactic coordinates AP: 1.3-1.5 mm, Lat: 0.4-0.6 mm, DV: 3.9-4.3). The voltammetric electrodes consisted of one 30- μ m diameter carbon fiber coated with Nafion (Aldrich, Milwaukee, WI). Electrochemical measurements were performed using a high-speed chronoamperometric apparatus (Quanteon, Lexington, KY) as previously described.¹² DA release was evoked by local injections of 200-300 nl of KCl (120 mM) at 10-min intervals in the presence or absence of the mGLUR broad-spectrum antagonist LY341495 (100 μ M). The results are presented as the mean \pm SEM of the difference in maximal DA variation after KCl ejection. The differences in DA release between the different groups of mice were assessed as a comparison to the differences in maximal variation for each group. The time to reach 80% of the maximal response (t80) was measured as an estimate of DA clearance.

Electrophysiological *in vivo* recording of VTA neurons

In vivo electrophysiological recordings of VTA neurons were performed as previously described.¹³ For recordings of VTA neurons, extracellular recording electrodes were constructed from borosilicate glass tubing (1.5 mm O.D./1.17 mm I.D., Harvard Apparatus, UK) using a vertical electrode puller (Narishige, JAPAN). Tips were broken, and electrodes were filled with a

0.5% Na-acetate solution yielding impedances of 6-9 M Ω . Animals were anesthetized with chloral hydrate (400 mg/kg, *i.p.*, supplemented as required to maintain optimal anesthesia throughout the experiment) and placed in a stereotaxic apparatus (Kopf instrument, CA, USA). The left saphenous vein was catheterized for the intravenous administration of cocaine, and the right saphenous vein was catheterized for the intravenous administration of quinpirole and eticlopride. The electrophysiological activity was sampled in the central region of the VTA (coordinates: between 3.1 to 3.5 mm posterior to Bregma, 0.3 to 0.6 mm lateral to midline, and 4 to 4.7 mm below brain surface). Spontaneously active DAergic neurons were identified on the basis of previously established electrophysiological criteria: 1) a typical triphasic action potential with a marked negative deflection; 2) a characteristic long duration (>2.0 ms); 3) an action potential width from start to negative trough of >1.1 ms; and 4) a slow firing rate (between 1 and 10Hz) with an irregular single spiking pattern and occasional short, slow bursting activity.^{14; 15} At least 5 min of spontaneous baseline electrophysiological activity was recorded before the intravenous injection of cocaine (1 mg/kg). Fifteen min after the first cocaine injection, quinpirole (1 mg/kg) was administered intravenously. Five min later, eticlopride (1 mg/kg) was administered intravenously. For each cell, the firing frequency was rescaled as a percentage of its baseline value averaged over the 2 min before cocaine injection. The effect of cocaine was assessed as a comparison between the maximum variation of the firing rate and the spike within burst (SWB) observed during the first 2 min after saline or cocaine injections. The analysis of the DAergic neurons' firing pattern was processed as previously described.¹³ The results are presented as the mean \pm SEM of the difference in the maximal variation before and after cocaine. The differences in cocaine effects between the groups were assessed as a comparison between the differences in maximal variation for each group. We used a Student's t test when both parameters followed a normal distribution (Shapiro test, $p>0.05$) and a non-parametric Mann-Whitney test when they did not, as mentioned in the figure legends.

Electrophysiological *in vitro* recording of MSN

In vitro recordings of MSN were performed as previously described.^{16; 17} WT (n=6), WT:DRD1a-EGFP (n=8), VGLUT3^{-/-} (n=8) and VGLUT3^{-/-}:DRD1a-EGFP mice (n=10) (3 to 4 weeks old) were anesthetized (150 mg/kg ketamine/10 mg/kg xylazine) for slice preparation. Coronal 300- μ m slices were prepared in bubbled ice-cold 95% O₂/5% CO₂-equilibrated solution containing the following (in mM): 110 choline Cl; 25 glucose; 25 NaHCO₃; 7 MgCl₂; 11.6 ascorbic acid; 3.1 Na⁺ pyruvate; 2.5 KCl; 1.25 NaH₂PO₄; and 0.5 CaCl₂. The slices were then stored at room temperature in 95% O₂/5% CO₂-equilibrated artificial cerebrospinal fluid (ACSF) containing the following (in mM): 124 NaCl; 26.2 NaHCO₃; 11 glucose; 2.5 KCl; 2.5 CaCl₂; 1.3 MgCl₂; and 1 NaH₂PO₄. The slices were kept at 32-34°C in a recording chamber superfused with 2.5 ml/min ACSF. Visualized whole-cell voltage-clamp recording techniques were used to measure the holding current and synaptic responses of MSNs of the nucleus accumbens shell with an upright microscope (Olympus France). Currents were amplified, filtered at 5 kHz and digitized at 20 kHz and recorded at a holding potential of -70 mV (IGOR PRO, Wavemetrics, USA). Access resistance was monitored using a step of -10 mV (0.1 Hz), and experiments were discarded if the access resistance increased by more than 20%. Miniature EPSCs were recorded at V_h=-60 mV in the presence of tetrodotoxin (0.5 μ M) using an internal solution containing the following (in mM): 140 potassium gluconate, 4 NaCl, 2 MgCl₂, 1.1 EGTA, 5 HEPES, 2 Na₂ATP, 5 sodium creatine phosphate, and 0.6 Na₃GTP (pH 7.3 with KOH). The frequency, amplitude and kinetic properties of these currents were then analyzed using the Mini Analysis software package (Synaptosoft, Decatur, GA, USA). Synaptic currents were evoked by stimuli (60 μ s) at 0.1 Hz through a glass pipette placed 200 μ m from the patched neurons. The internal solution contained (in mM): 130 CsCl, 4 NaCl, 2 MgCl₂, 1.1 EGTA, 5 HEPES, 2 Na₂ATP, 5 sodium creatine phosphate, 0.6 Na₃GTP and 0.1 spermine. All experiments were performed in the

presence of bicuculline (20 μ M). α -amino-3-hydroxy-5-methyl-4-isoxazole propionic acid (AMPA):N-methyl-D-aspartate (NMDA) ratios of evoked excitatory postsynaptic currents (EPSCs) were obtained by evoking pure AMPA-EPSC at -60 mV and a mix of AMPA and NMDA at +40 mV. The NMDA component was extracted at 30-50 ms from EPSC onset when the AMPA component was back at baseline.¹⁶

Online/offline analyses were performed using IGOR-6 (Wavemetrics, USA) and Prism (GraphPad, USA). Compiled data are expressed as the mean \pm SEM. Significance was set at $\alpha=0.05$ using Student's t-test and the Kolmogorov-Smirnov (KS) test.

DRD1 and DRD2 autoradiography

Auto-radiographic detection of DRD1 and DRD2 was performed as previously described.⁴ In short, fresh frozen sections of mice brains (WT n=5; VGLUT3^{-/-} n=5) were pre-incubated in 50 mM Tris-HCl Buffer, pH 7.4-7.5, with 120 mM NaCl, 5 mM KCl, 2 mM CaCl₂ and 1 mM MgCl₂. Then, the sections were incubated with either [³H]SCH23390 (for DRD1 labeling) or [¹²⁵I]iodosulpride (DRD2 labeling), both of which were purchased from GE Healthcare. [³H]SCH23390-labeled sections were exposed to BAS-TR Fuji Imaging screens (Fuji Film Photo Co., Tokyo, Japan). Screens were then scanned with a Fuji Bioimaging Analyzer BAS-5000 (Fuji Film Photo Co., Tokyo, Japan). [¹²⁵I]iodosulpride-labeled sections were exposed to X-ray films (Biomax MR, Eastman Kodak), scanned and converted to 16-bit images using a Umax PowerLook 1100 scanner (Umx System, Willich, Germany). Digitized images were analyzed with MCID software (Imaging Research, St. Catharine's, ON, Canada). The results are expressed as the mean \pm SEM. of optical density (in arbitrary units).

Immunofluorescence

Mice were anesthetized and intracardially perfused with PBS containing 4% paraformaldehyde (PFA). Brains were dissected, post-fixed by immersion in the same fixative and cryoprotected in PBS containing 10% sucrose. Coronal sections (20 μ m) were cut using a vibratome and stored at -20°C in cryoprotective solution until use. Immunofluorescence was performed on free-floating sections as previously described.¹⁸ Sections were incubated with VGLUT3 rabbit antiserum (1:2,000, Synaptic Systems, catalog ref 135-203),⁴ serotonin rat monoclonal antiserum (1:50, Millipore Bioscience Research Reagents, catalog ref AB12), and home-made VAcHT guinea pig antiserum (1:5,000).⁴ Primary antibodies were detected with anti-rabbit, anti-guinea pig or anti-mouse IgG coupled to Alexa Fluor 488, Alexa Fluor 555 or Cy5 (1:2,000, Invitrogen). Slices were mounted on glass slides with Fluoromount-G (Southern-Biotech). Images were acquired using a Confocal Laser Scanning Microscope (Leica TCS SP5 AOBS, Leica Microsystems, Mannheim, Germany) equipped with a 63x, 1.4 NA oil immersion objective with the pixel size set to 60 nm and a z-step of 130 nm. Images were deconvoluted using a Maximum Likelihood Estimation algorithm with Huygens 3.6 software (Scientific Volume Imaging). Settings were used such that background intensity was averaged from the voxels with lowest intensity and the signal to noise ratio was estimated to a value of 20. Labeled terminals were quantified using the 3D object counter plugin for ImageJ.¹⁹ Co-localization analysis was performed based on the correlation of intensities between pairs of pixels in the two different channels as described by Jaskolski et al. (2005)²⁰ using the colocalization color map plugin for ImageJ. Super-resolution imaging of sub-synaptic clusters of material enriched for VGLUT3 or VAcHT or both was revealed with Structured Illumination Microscopy (Nikon N-SIM; Nikon Imaging Center at Institut Curie, Paris, France).

Diolistic labeling and dendritic spine analysis

Mice (WT n=11; VGLUT3^{-/-} n=14) were anesthetized with pentobarbital, and a fast (2-min)

transcardial perfusion with 30 ml of PFA (1.5% in PBS) was performed. The brains were removed and post-fixed for 1 h in the same fixative, and sections (150 μ m) were cut with a vibratome.²¹ Image stacks of MSN dendrites were acquired in the NAc shell using a 488 or 561-nm laser line for excitation of a Confocal Laser Scanning Microscope (SP5, Leica). Image stacks were deconvoluted with Huygens 3.5 software (Scientific Volume Imaging). NeuronStudio software was used to analyze dendritic spines.²² After automated detection, manual checks were performed to avoid false positives.

Statistics

All statistical comparisons were performed with two-sided tests with Prism 5 (GraphPad Software, Inc.). Mann Whitney tests, one-way and repeated measures two-way ANOVA were used when appropriate. Bonferroni's test for multiple comparisons post-hoc analysis was performed when required unless otherwise indicated.

In the case of sensitization, the statistical analysis was performed using StatView (SAS Institute Inc.). A three-way ANOVA with repeated measures was used followed by Tukey's/Kramer's test as a post-hoc test.

All results are expressed as the mean \pm SEM, and differences were considered significant at $p < 0.05$.

RESULTS

VGLUT3 deletion exacerbates cocaine-induced behaviors

In the NAc, TANs express VGLUT3 in addition to VAcHT (Supplementary Figure S1). To assess whether VGLUT3 influences NAc-driven behaviors, we explored cocaine-related endophenotypes in VGLUT3^{-/-} mice and WT littermates. Silencing of VGLUT3 resulted in marked cocaine-induced locomotor activity (Supplementary Figure S2),⁴. Sensitization to repeated cocaine administration²³ was evaluated in VGLUT3^{-/-} and WT littermates (Figure 1a and b; Supplementary Table S1). WT mice displayed significantly higher levels of locomotor activity on the challenge day than on the first day of cocaine administration (Figure 1b). At the initial cocaine exposure, VGLUT3^{-/-} mice exhibited higher drug-induced locomotor activity than WT mice (+103%, $p < 0.05$). The cocaine-induced locomotor activity of the mutants remained similar on days 4 and 13. Thus, VGLUT3 deletion induced an immediate increase in cocaine-induced locomotor activity but occluded further sensitization to cocaine.

In addition to its locomotor effects, cocaine has reinforcing properties. The affective state in a drug-paired environment can be modeled in rodents using the conditioned place preference (CPP) test.²⁴ VGLUT3^{-/-} mice, unlike WT littermates, showed a marked CPP at the lowest dose of cocaine (2.5 mg/kg, $p = 0.003$, Figure 1c). No difference in CPP was observed for the two genotypes at a higher dose of cocaine (5 mg/kg). Thus, reinforcing properties of cocaine were increased by VGLUT3 deletion in CPP.

To further evaluate the reinforcing properties of psychostimulant drugs in VGLUT3^{-/-} mice, we used the operant cocaine self-administration paradigm. During both FR1 and FR3, more VGLUT3^{-/-} mice than WT mice met the acquisition criteria for the cocaine-maintained operant response (Supplementary Figure S3). Throughout the training, VGLUT3^{-/-} animals showed more active nose-poking responses than WT littermates (Figure 1d and e; Supplementary Table S2).

Animals were then tested in a progressive ratio (PR) schedule. The breaking point values were significantly higher in VGLUT3^{-/-} mice (76.77±9.69 nose pokes) than in WT mice (45.14±7.49 nose pokes) (Figure 1f). Thus, VGLUT3^{-/-} mice appeared to experience an enhanced motivation for cocaine. Following FR1, FR3 and the PR schedule, animals underwent extinction of operant responses to cocaine for 18 days. Responses of mutant mice at the active hole were comparable to those of WT mice and decreased across sessions in both genotypes (Figure 1d and e; Supplementary Table S2). After the 18 days of forced cocaine abstinence, mice were evaluated for cue-induced reinstatement of cocaine-seeking behavior. In this test, active nose-poking responses were significantly more pronounced in VGLUT3^{-/-} mice than in WT littermates (Figure 1g) in a drug-associated environment.

Overall, VGLUT3^{-/-} mice experienced a higher level of acquisition of self-administration, improved FR1 and FR3 performance, and had comparable levels of extinction. Furthermore, mice lacking VGLUT3 appeared to be more vulnerable to relapse. However, relapse vulnerability should be interpreted with caution given that VGLUT3^{-/-} mice demonstrated a confounding higher degree of response with all schedules tested and with a higher PR breakpoint.

Dual regulation of dopamine release by TANs in the NAc

DA transmission is critical for enabling the reinforcing properties of cocaine. Using *in vivo* voltammetry, we measured the release of DA in response to KCl-induced depolarization in the NAc of VGLUT3^{-/-} and WT mice. A single KCl pulse evoked a transient release of DA that was significantly higher in VGLUT3^{-/-} mice than in WT animals (Figure 2a and b, +96%, $p=0.001$). No significant modification was observed in the clearance of extracellular DA at T80 (Figure 2c), indicating that DA reuptake was unaltered in VGLUT3^{-/-} mice. *In vivo* electrophysiological recordings in VTA showed that this increased DA release was not related to a modified firing nor to an altered sensitivity to cocaine of DA neurons (Supplementary Figure S4).

TANs signal with both ACh and glutamate, and the synaptic storage of ACh is decreased in VGLUT3-null mice.^{4; 5} To further dissect the specific roles of ACh and glutamate in TANs, we tested DA release in mice without the ability to release ACh in the striatum due to selective elimination of VAcHT.⁶ In VAcHT^{D2-Cre-flox/flox} mice, the amplitude of the KCl-induced DA release was markedly lower than in WT mice (Figure 2a and b, -69%, $p=0.00006$). No difference in T80 was observed for the two genotypes (Figure 2c). Thus, glutamate and ACh originating from TANs had opposing effects on DA efflux.

The electrochemical detection of DA by *in vivo* voltammetry reflects the dynamic balance between DA release, DA reuptake and DA receptor D2 (DRD2) presynaptic inhibition of release.²⁵ To investigate the functional consequences of the lack of VGLUT3 or VAcHT on the DRD2-dependent accommodation of the response, the DA max release as well as the T80 were compared after four consecutive KCl ejections (K1-K4, Figure 2b and 2c) administered at 10-min intervals. As expected, repeated KCl ejections resulted in a progressive decline in responses for all three genotypes. After each successive depolarization, the DA release was always significantly higher in the NAc of VGLUT3^{-/-} mice and lower in VAcHT^{D2-Cre-flox/flox} mice than in WT mice. The DRD2 regulation appeared unaltered in these mutant mouse lines.

Consistent with their increased cocaine-self administration, VGLUT3^{-/-} mice demonstrated a marked enhancement of DA efflux in the NAc. Thus, we explored whether this finding might be related to local effects in the NAc. Local application of a metabotropic glutamate receptor (mGLUR) antagonist has been shown to increase DA release in the NAc.²⁶ We thus investigated whether glutamate originating from TANs could exert a local inhibition of DA release by binding to mGLURs. As shown in Figure 2d and e, DA efflux was significantly increased by the local application of the broad-spectrum antagonist mGLUR LY341495²⁷ in WT mice (+96%, $p=0.00006$) but not in VGLUT3^{-/-} mice. Therefore, blocking mGLUR had the same net effect on

DA release as deleting VGLUT3. These findings suggest that VGLUT3-dependent glutamate release by TANS in the NAc of WT mice inhibits DA efflux by activating mGLUR.

The DA receptor D1 signaling cascade was activated in the NAc of VGLUT3^{-/-} mice

The augmented behavioral response to cocaine and the increased DA release in the NAc of VGLUT3^{-/-} mice prompted us to investigate the status of dopaminergic signaling cascades. The density of DRD2 binding sites did not differ between VGLUT3^{-/-} and WT mice (Figure 3a). However, the density of DRD1 was significantly higher in the NAc of VGLUT3^{-/-} mice (Figure 3b, +41%, $p=0.03$) but not in their dorsal striatum.

Cocaine-triggered DA release activates extracellular signal-regulated kinase (ERK) in DRD1-positive MSNs.²⁸ The activation of ERK following acute cocaine injection was monitored in the NAc and the dorsal striatum of VGLUT3^{-/-} and WT littermates (Figure 3c). Interestingly, following a 2.5 mg/kg injection of cocaine, the number of phosphorylated ERK-positive cells was significantly higher in the NAc of VGLUT3^{-/-} mice (+44%, $p<0.05$) than of WT mice (Figure 3c). At this dosage, no difference was observed between the dorsal striata of WT and mutants. A 10 mg/kg dose of cocaine caused a similar increase in phosphorylated ERK-positive neurons in the dorsal and ventral striata of both genotypes. Therefore, DRD1 receptor density and the ERK pathway were upregulated in the NAc of VGLUT3^{-/-} mice.

VGLUT3 regulates morphological and functional properties of excitatory synapses onto MSNs

The cocaine-induced activation of the DRD1 cascade results in structural modifications of MSNs.^{8; 32; 33} Therefore, we explored how chronic cocaine treatment may affect the remodeling of dendritic spines in the NAc of VGLUT3^{-/-} and WT mice (Figure 3d). Spine density was

measured in the NAc of saline-treated or cocaine-sensitized mice (as described in Figure 1a). As expected, spine density was significantly increased after cocaine sensitization in the MSNs of the NAc of WT animals (+50%, $p=0.006$). Surprisingly, the spine density of saline-injected VGLUT3^{-/-} mice was comparable to that of cocaine-treated WT or VGLUT3^{-/-} mice. Therefore, MSNs from the NAc of VGLUT3^{-/-} mice presented constitutively elevated spine densities.

Glutamatergic afferents originating from the cortex, the thalamus, the hippocampus or the amygdala converge onto the spines of MSN from NAc to regulate reward behaviors.^{34; 35} Thus, we investigated whether glutamatergic nerve endings were also modified in the NAc of VGLUT3^{-/-} mice. Interestingly, post-synaptic changes were not accompanied by presynaptic modifications of VGLUT1 or VGLUT2 levels, either locally in the NAc or distally in the prefrontal cortex (Figure 3e and f).

Long-lasting changes in spine numbers are hypothesized to contribute to persistent synaptic adaptations³³. The observed changes in spine number led us to perform whole-cell patch-clamp recordings from MSNs of the NAc (shell) of WT or VGLUT3^{-/-} mice (Figure 3 g-k). To probe for synaptic adaptations in the mutants, we evoked AMPA-receptor mediated responses at -60 mV and a mixture of AMPA and NMDA-receptor mediated responses at +40 mV. We compared the relative contribution of AMPA versus NMDA receptors to evoke EPSCs. The NMDA receptor-mediated component was computed by measuring the amplitude at +40 mV 30-50 ms after the onset of the EPSC. We detected a significantly higher AMPA/NMDA ratio in mutant mice than in WT mice (Figure 3g, $p=0.02$). To further examine the regulation of excitatory transmission in the NAc shell, we measured miniature EPSCs (mEPSCs, Figure 3h-j). VGLUT3^{-/-} mice demonstrated significantly increased mEPSCs frequency of AMPA-receptor mediated currents (Figure 3i, $p=0.007$). However, no alterations in the mEPSC amplitude (Figure 3j) nor in the paired-pulse ratio of evoked EPSCs (Figure 3k) were detected in VGLUT3^{-/-} mice, which suggests the absence of presynaptic modifications and is consistent with an increased spine

number. The strengthening of glutamatergic transmission in the mutants did not prevent cocaine-evoked plasticity of excitatory transmission. Indeed, as previously reported,³⁶ 24 hours after the last cocaine injection, AMPA/NMDA ratios were reduced compared to saline-treated mice in both WT and VGLUT3^{-/-} (Figure S5). These morphological and electrophysiological changes suggest that glutamatergic transmission in the NAc is strengthened in the absence of VGLUT3 but is still sensitive to cocaine exposure.

Cocaine experience modifies excitatory transmission specifically at glutamatergic synapses onto D1-positive MSNs.³⁷ To test whether VGLUT3 deletion-induced modifications are neuron-specific, we crossed VGLUT3^{-/-} mice with *Drd1a*-EGFP mice. This allowed us to visualize DRD1-positive neurons and discriminate them from other neuronal subtypes in the NAc. Using these double mutants, we found that the numbers of DRD1-positive and DRD1-negative MSNs were similar in the brains of WT and VGLUT3^{-/-} mice (Figure 4a). Therefore, the augmented DRD1 binding site density (depicted on Figure 3b) was not related to an increased number of DRD1 and DRD1/DRD2-positive MSNs in the NAc. Furthermore, we found that the increased spine density reported in the NAc of VGLUT3^{-/-} mice (see Figure 3d) was restricted to DRD1-positive MSNs (+63% in GFP-positive MSNs, $p=0.0003$, Figure 4b). In contrast, no significant changes in spine density were observed in DRD1-negative MSNs (putatively DRD2-positive MSNs, Figure 4b). Consistent with the morphological modifications of D1-MSNs in VGLUT3^{-/-}:*Drd1a*-EGFP mice, we found that AMPA/NMDA ratios were higher in the absence of VGLUT3 (Figure 4c-e). AMPA/NMDA ratios were comparable in EGFP-negative MSNs recorded from WT and VGLUT3^{-/-} (Figure 4c-e). Taken together, these data suggest that the absence of VGLUT3 specifically modifies morphology as well as glutamatergic transmission onto DRD1-positive striato-nigral MSNs.

The frequency of rare variations in *SLC17A8* is increased in patients with severe addiction

Behavioral, biochemical, morphological and physiological analyses demonstrated that in the absence of VGLUT3, mice were more vulnerable to cocaine. These results suggest that allelic variations in VGLUT3 might be correlated with drug-seeking behavior in humans. Therefore, we sought rare mutations in the *SLC17A8* gene in a population of 230 patients with severe addiction to cocaine or opiates. We identified seven mutations that predict an amino acid change in the protein sequence and two synonymous variations (Figure 4, **Table 1** and Table S4). One of these variations (p.T8I) was found in 6 non-related subjects. All mutations affected amino acids that were highly conserved throughout evolution (average conservation of 0.973 in 16 vertebrate species). Five of these six amino acids (p.G71S, p.V104I, p.G130D, p.Y252S and p.P443L) were also conserved in VGLUT1 and VGLUT2 and predicted to be essential for the function of the VGLUT3 protein (Table S4). None of the missense mutations were found in 213 control subjects of French origin without addiction, psychiatric disorder or suicidal behavior. In this control group, we identified only one missense mutation (p.V185I) and one synonymous variation (p.S410), suggesting that mutated alleles were significantly more frequent in subjects with severe addiction than in controls (2.6% and 0.2%, respectively, Fisher's exact test odds ratio=11.1, 95%CI[1.4;86.0], $p=0.003$) (**Table 1**). We examined the mutation frequency observed in the 1000 Genomes Project.³⁸ Out of the 1,092 subjects sequenced through phase 1, 8 missense variations were reported in 26 subjects and 10 synonymous variations were identified in 145 subjects (**Table 1**). Again, this demonstrated that the mutated allele frequency was significantly higher in subjects with severe addiction compared with the general population from the 1000 Genomes Project (2.6% and 1.2%, respectively, Fisher's exact test odds ratio=2.2, 95%CI[1.1;4.4], $p=0.03$). We compared the non-synonymous and synonymous substitution rates between the patient and control populations using the ratio of the number of non-synonymous

substitutions per non-synonymous site (d_N) to the number of synonymous substitutions per synonymous site (d_S) as an indicator of selective pressure acting on VGLUT3 (Figure S6a). Interestingly, whereas the d_N/d_S ratio suggested a strong negative selection against *SLC17A8* in general population ($d_N/d_S=0.23$), this ratio was 4-fold higher ($d_N/d_S=0.99$) in the population of subjects with severe addiction, confirming the higher number of amino acid substitutions in this population compared with synonymous variations. To confirm our observations, we used a replication cohort of 265 opiate dependent patients in methadone maintenance treatment from Switzerland, some with cocaine addiction. This mutation screening identified 4 new amino acid changes and 2 synonymous variations (Figure 4, Table 1 and Table S4), giving a mutation frequency of 0.8%. Although this frequency was higher than both of the frequencies observed in our French control population (0.2%) and in European subjects from the 1000 Genomes Project (0.5%), these differences were not significant (Fisher's exact test $p=0.39$ and $p=0.72$, respectively). However, we again noted a higher d_N/d_S ratio ($d_N/d_S=0.57$) in the cohort from Switzerland than in the 1000 Genomes Project, confirming the increased frequency of non-synonymous variations in subjects with severe addiction.

Among the mutations identified in the cohort of subjects with severe addiction, one involved a change from a threonine at position 8 to an isoleucine [c.21C>T(p.T8I), rs45610843] and was found in six independent subjects. Five of these patients were of African origin, and one had two grandparents from Asia and two grandparents from Europe. To determine whether this variant was an ethnic-specific polymorphism or might be overrepresented in the population of patients with severe addiction, we screened the first exon of *SLC17A8* in 390 additional control subjects from Africa and compared the frequency of this allele in patients of identical origin. The I8 allele was found in 12 control subjects, revealing an allele frequency of 1.8% in the African population. This was consistent with the 1.2% frequency reported in subjects of African origin from the 1000 Genomes Project phase 1 (Figure S6b; Fisher's exact test odds ratio=1.2, 95%CI[0.4;4.1],

$p=0.81$). Interestingly, the I8 allele was found at a frequency of 5.1% in patients of African origin with severe addiction, suggesting that this polymorphism was significantly overrepresented in patients with substance use disorders (Fisher's exact test odds ratio=3.8, 95%CI[1.1;10.9], $p=0.02$) and increased the risk of addiction by a factor of three. Therefore, our results suggest that mutations that potentially alter VGLUT3 activity are associated with severe addiction in humans, a result that is consistent with the increased sensitivity to cocaine in VGLUT3-null mice.

DISCUSSION

It is well established that DA input from the VTA and local cholinergic TANS critically regulates reward-guided behaviors. DAergic and cholinergic neurons exhibit a characteristic alteration in pause-rebound activity in response to salient stimuli that is tightly controlled by GABAergic afferents from the VTA.^{39; 40} However, how TANS control the accumbal microcircuit is far from fully understood. In particular, little is known about the dual co-release of glutamate and Ach in the regulation of reward behavior.

The present study provides evidence that VGLUT3 blunts cocaine behaviors by regulating DA and glutamate signaling in the NAc. TANS from the NAc have long been recognized as key regulators of reward behavior and of the reinforcing properties of cocaine.^{41; 42} However, the mechanism by which TANS operate remains a matter of debate.⁴³ Our study suggests that one key to understanding this critical question resides in the fact that TANS use two different chemical codes to communicate with surrounding neural networks in the NAc: ACh and glutamate. We found that mice lacking Ach-release in the NAc exhibit a decreased DA release. This is consistent with previous observations showing that nicotinic ACh receptors (nAChR) exert stimulatory control over DA efflux (for review see ⁴⁴). However, silencing ACh transmission in TANS minimally influenced reward behaviors,⁶ and the marked decreased DA transmission in VAcHT-null mice did not translate into a decrease in reward behavior. These observations will require further investigation.

In contrast, we herein report for the first time that TANS use VGLUT3-dependent glutamate and mGLURs to diminish DA release in the NAc and to modulate the reinforcing properties of cocaine. A negative regulation of DA release exerted by mGLURs in the NAc was previously reported²⁶; however, the source of glutamate was not clearly identified. We herein establish that the stimulatory effects of a broad-spectrum mGLUR antagonist (LY341495) on DA efflux are observed exclusively in WT mice but not VGLUT3^{-/-} mice. Therefore, this mGLUR negative

regulation of DA release is not influenced by glutamate coming from cortical or thalamic glutamatergic inputs but appeared to be strictly TANs- and VGLUT3-dependent.

It is now well established that TANS optogenetic stimulation results in monosynaptic glutamate- and acetylcholine-mediated currents in striatal MSN and fast-spiking GABAergic interneurons (FSI).^{5; 45} Our results establish that glutamate/ACh co-transmission from TANs controls not only MSN and FSI but DA terminals as well.

The absence of VGLUT3 resulted in an increase in DA release with a concomitant activation of the pro-reward DRD1 signaling cascade. The augmented activity of DRD1-positive MSNs has been shown to promote reinforcement of behaviors in contrast to DRD2-positive MNS, which induce punishment.^{29-31; 46} Furthermore, VGLUT3 null mice demonstrated increased spine density and augmented glutamatergic signaling in the NAc. Interestingly, deletion of VGLUT3 appeared to exclusively affect the DRD1 pro-reward pathway without affecting DRD2-positive MNS. Therefore, the constitutive absence of VGLUT3 appears to produce the same effects as sustained cocaine intake. Excitatory cortical transmission is believed to encode for learning and the unmanageable motivation to seek drugs, whereas DA codes reward prediction and the “wanting” of a drug.⁴⁷⁻⁴⁹ Thus, with VGLUT3 and glutamate/ACh co-transmission, TANs use sophisticated machinery to shape accumbal dopaminergic and glutamatergic signals and thereby orchestrate reward seeking. The major findings of the present study are summarized in Figure 6.

Whether observations made in mouse models are relevant to humans remains to be fully established. Humans are not equivalent in their response to addictive drugs, and only a small percentage of susceptible individuals develop cocaine addiction.⁵⁰ Genetic variants may play an important role in the susceptibility to drug addiction. Given our observations, we hypothesize that allelic variations in VGLUT3 may contribute to the vulnerability of a subgroup of individuals who demonstrate heavy drug use. It is possible that VGLUT3 mutations may contribute to a

presensitized reward circuit in humans as well. In support of this working hypothesis, we report that the frequency of rare variations within the gene encoding VGLUT3 is higher in individuals with substance use disorders than in controls.

VGLUT3 is discretely distributed throughout the brain and may therefore be a relevant pharmacological target to treat addiction or other striatum-related diseases. A deeper understanding of the contributions of VGLUT3 to reward behaviors could pave the way for developing new therapeutic strategies for drug abuse or to allow the identification of individuals vulnerable to drug-seeking behavior.

ACKNOWLEDGMENTS

This research was supported by funds from ANR (ANR-09-MNPS-033, ANR-13-SAMA-0005-01), *Équipe* FRM DEQ20130326486, FRC, Brain Canada Multi-Investigator Research Initiative, Djavad Mowafaghian Foundation, ERANET-Neuron Joint Transnational Call for "European Research Projects on Mental Disorders", INSERM, CNRS and UPMC. The research teams of SEM, SJ, MM, JC-PV, BG and FB are members of the Bio-Psy Laboratory of Excellence; this work was therefore supported by French state funds managed by the ANR within the *Investissements d'Avenir* program under reference ANR-11-IDEX-0004-02. DYS was funded by the École des Neurosciences de Paris. This work was also supported by the City of Paris and Inserm Atip-Avenir to MM. FV was supported by grants from the *Mission Interministérielle de Lutte contre la Drogue et la Toxicomanie* (MILDT, 2006); the *Département de la Recherche Clinique et du Développement-Assistance Publique Hôpitaux de Paris* (DRCD-APHP, OST07013); and from the *Programme Hospitalier de Recherches Cliniques* (PHRC program, AOM10165). The Cellular Imaging and Flow Cytometry Facility is supported by the Conseil Régional Ile-de-France. We thank Emily Nichols for recruiting patients and data analysis. We also thank Dr. Ryad Tamouza for providing DNA sample controls from Africa.

Supplementary information is available at *Molecular Psychiatry's* website

CONFLICT OF INTEREST

The authors declare no conflicts of interest.

REFERENCES

1. Di Chiara G, Imperato A. Preferential stimulation of dopamine release in the nucleus accumbens by opiates, alcohol, and barbiturates: studies with transcerebral dialysis in freely moving rats. *Ann N Y Acad Sci* 1986; **473**: 367-381.
2. Kalivas PW, Volkow ND. The neural basis of addiction: a pathology of motivation and choice. *Am J Psychiatry* 2005; **162**(8): 1403-1413.
3. Luscher C, Ungless MA. The mechanistic classification of addictive drugs. *PLoS Med* 2006; **3**(11): e437.
4. Gras C, Amilhon B, Lopicard EM, Poirel O, Vinatier J, Herbin M *et al.* The vesicular glutamate transporter VGLUT3 synergizes striatal acetylcholine tone. *Nature neuroscience* 2008; **11**(3): 292-300.
5. Higley MJ, Gittis AH, Oldenburg IA, Balthasar N, Seal RP, Edwards RH *et al.* Cholinergic interneurons mediate fast VGLUT3-dependent glutamatergic transmission in the striatum. *PLoS One* 2011; **6**(4): e19155.
6. Guzman MS, De Jaeger X, Raulic S, Souza IA, Li AX, Schmid S *et al.* Elimination of the vesicular acetylcholine transporter in the striatum reveals regulation of behaviour by cholinergic-glutamatergic co-transmission. *PLoS Biol* 2011; **9**(11): e1001194.

7. Crettol S, Deglon JJ, Besson J, Croquette-Krokar M, Hammig R, Gothuey I *et al.* ABCB1 and cytochrome P450 genotypes and phenotypes: influence on methadone plasma levels and response to treatment. *Clin Pharmacol Ther* 2006; **80**(6): 668-681.
8. Besnard A, Bouveyron N, Kappes V, Pascoli V, Pages C, Heck N *et al.* Alterations of molecular and behavioral responses to cocaine by selective inhibition of Elk-1 phosphorylation. *The Journal of neuroscience : the official journal of the Society for Neuroscience* 2011; **31**(40): 14296-14307.
9. Martin-Garcia E, Barbano MF, Galeote L, Maldonado R. New operant model of nicotine-seeking behaviour in mice. *Int J Neuropsychopharmacol* 2009; **12**(3): 343-356.
10. Soria G, Barbano MF, Maldonado R, Valverde O. A reliable method to study cue-, priming-, and stress-induced reinstatement of cocaine self-administration in mice. *Psychopharmacology* 2008; **199**(4): 593-603.
11. Soria G, Mendizabal V, Tourino C, Robledo P, Ledent C, Parmentier M *et al.* Lack of CB1 cannabinoid receptor impairs cocaine self-administration. *Neuropsychopharmacology : official publication of the American College of Neuropsychopharmacology* 2005; **30**(9): 1670-1680.

12. Richardson NR, Gratton A. Changes in nucleus accumbens dopamine transmission associated with fixed- and variable-time schedule-induced feeding. *The European journal of neuroscience* 2008; **27**(10): 2714-2723.
13. Tolu S, Eddine R, Marti F, David V, Graupner M, Pons S *et al.* Co-activation of VTA DA and GABA neurons mediates nicotine reinforcement. *Molecular psychiatry* 2013; **18**(3): 382-393.
14. Grace AA, Bunney BS. Intracellular and extracellular electrophysiology of nigral dopaminergic neurons--1. Identification and characterization. *Neuroscience* 1983; **10**(2): 301-315.
15. Grace AA, Bunney BS. The control of firing pattern in nigral dopamine neurons: burst firing. *The Journal of neuroscience : the official journal of the Society for Neuroscience* 1984; **4**(11): 2877-2890.
16. Mameli M, Bellone C, Brown MT, Luscher C. Cocaine inverts rules for synaptic plasticity of glutamate transmission in the ventral tegmental area. *Nature neuroscience* 2011; **14**(4): 414-416.
17. Mameli M, Halbout B, Creton C, Engblom D, Parkitna JR, Spanagel R *et al.* Cocaine-evoked synaptic plasticity: persistence in the VTA triggers adaptations in the NAc. *Nature neuroscience* 2009; **12**(8): 1036-1041.

18. Amilhon B, Lepicard E, Renoir T, Mongeau R, Popa D, Poirel O *et al.* VGLUT3 (vesicular glutamate transporter type 3) contribution to the regulation of serotonergic transmission and anxiety. *The Journal of neuroscience : the official journal of the Society for Neuroscience* 2010; **30**(6): 2198-2210.
19. Bolte S, Cordelieres FP. A guided tour into subcellular colocalization analysis in light microscopy. *J Microsc* 2006; **224**(Pt 3): 213-232.
20. Jaskolski F, Mulle C, Manzoni OJ. An automated method to quantify and visualize colocalized fluorescent signals. *Journal of neuroscience methods* 2005; **146**(1): 42-49.
21. Heck N, Betuing S, Vanhoutte P, Caboche J. A deconvolution method to improve automated 3D-analysis of dendritic spines: application to a mouse model of Huntington's disease. *Brain structure & function* 2012; **217**(2): 421-434.
22. Rodriguez A, Ehlenberger DB, Dickstein DL, Hof PR, Wearne SL. Automated three-dimensional detection and shape classification of dendritic spines from fluorescence microscopy images. *PLoS One* 2008; **3**(4): e1997.
23. Sanchis-Segura C, Spanagel R. Behavioural assessment of drug reinforcement and addictive features in rodents: an overview. *Addict Biol* 2006; **11**(1): 2-38.

24. Carboni E, Vacca C. Conditioned place preference. A simple method for investigating reinforcing properties in laboratory animals. *Methods Mol Med* 2003; **79**: 481-498.
25. Schmitz Y, Benoit-Marand M, Gonon F, Sulzer D. Presynaptic regulation of dopaminergic neurotransmission. *J Neurochem* 2003; **87**(2): 273-289.
26. Karasawa J, Yoshimizu T, Chaki S. A metabotropic glutamate 2/3 receptor antagonist, MGS0039, increases extracellular dopamine levels in the nucleus accumbens shell. *Neuroscience letters* 2006; **393**(2-3): 127-130.
27. Fitzjohn SM, Bortolotto ZA, Palmer MJ, Doherty AJ, Ornstein PL, Schoepp DD *et al.* The potent mGlu receptor antagonist LY341495 identifies roles for both cloned and novel mGlu receptors in hippocampal synaptic plasticity. *Neuropharmacology* 1998; **37**(12): 1445-1458.
28. Bertran-Gonzalez J, Bosch C, Maroteaux M, Matamalas M, Herve D, Valjent E *et al.* Opposing patterns of signaling activation in dopamine D1 and D2 receptor-expressing striatal neurons in response to cocaine and haloperidol. *The Journal of neuroscience : the official journal of the Society for Neuroscience* 2008; **28**(22): 5671-5685.
29. Hikida T, Kimura K, Wada N, Funabiki K, Nakanishi S. Distinct roles of synaptic transmission in direct and indirect striatal pathways to reward and aversive behavior. *Neuron* 2010; **66**(6): 896-907.

30. Hikida T, Yawata S, Yamaguchi T, Danjo T, Sasaoka T, Wang Y *et al.* Pathway-specific modulation of nucleus accumbens in reward and aversive behavior via selective transmitter receptors. *Proc Natl Acad Sci U S A* 2013; **110**(1): 342-347.
31. Lobo MK, Nestler EJ. The striatal balancing act in drug addiction: distinct roles of direct and indirect pathway medium spiny neurons. *Front Neuroanat* 2011; **5**: 41.
32. Robinson TE, Kolb B. Alterations in the morphology of dendrites and dendritic spines in the nucleus accumbens and prefrontal cortex following repeated treatment with amphetamine or cocaine. *The European journal of neuroscience* 1999; **11**(5): 1598-1604.
33. Russo SJ, Dietz DM, Dumitriu D, Morrison JH, Malenka RC, Nestler EJ. The addicted synapse: mechanisms of synaptic and structural plasticity in nucleus accumbens. *Trends Neurosci* 2010; **33**(6): 267-276.
34. Heck N, Dos Santos M, Amairi B, Sallery M, Besnard A, Herzog E *et al.* A new automated 3D detection of synaptic contacts reveals the formation of cortico-striatal synapses upon cocaine treatment in vivo. *Brain structure & function* 2014.

35. Sesack SR, Grace AA. Cortico-Basal Ganglia reward network: microcircuitry. *Neuropsychopharmacology : official publication of the American College of Neuropsychopharmacology* 2010; **35**(1): 27-47.
36. Kourrich S, Rothwell PE, Klug JR, Thomas MJ. Cocaine experience controls bidirectional synaptic plasticity in the nucleus accumbens. *The Journal of neuroscience : the official journal of the Society for Neuroscience* 2007; **27**(30): 7921-7928.
37. Pascoli V, Turiault M, Luscher C. Reversal of cocaine-evoked synaptic potentiation resets drug-induced adaptive behaviour. *Nature* 2012; **481**(7379): 71-75.
38. Genomes Project C, Abecasis GR, Auton A, Brooks LD, DePristo MA, Durbin RM *et al.* An integrated map of genetic variation from 1,092 human genomes. *Nature* 2012; **491**(7422): 56-65.
39. Brown MT, Tan KR, O'Connor EC, Nikonenko I, Muller D, Luscher C. Ventral tegmental area GABA projections pause accumbal cholinergic interneurons to enhance associative learning. *Nature* 2012; **492**(7429): 452-456.
40. Tepper JM, Bolam JP. Functional diversity and specificity of neostriatal interneurons. *Current opinion in neurobiology* 2004; **14**(6): 685-692.

41. Hikida T, Kaneko S, Isobe T, Kitabatake Y, Watanabe D, Pastan I *et al.* Increased sensitivity to cocaine by cholinergic cell ablation in nucleus accumbens. *Proc Natl Acad Sci U S A* 2001; **98**(23): 13351-13354.
42. Kitabatake Y, Hikida T, Watanabe D, Pastan I, Nakanishi S. Impairment of reward-related learning by cholinergic cell ablation in the striatum. *Proc Natl Acad Sci U S A* 2003; **100**(13): 7965-7970.
43. Surmeier DJ, Graybiel AM. A feud that wasn't: acetylcholine evokes dopamine release in the striatum. *Neuron* 2012; **75**(1): 1-3.
44. Exley R, Cragg SJ. Presynaptic nicotinic receptors: a dynamic and diverse cholinergic filter of striatal dopamine neurotransmission. *Br J Pharmacol* 2008; **153 Suppl 1**: S283-297.
45. Nelson AB, Bussert TG, Kreitzer AC, Seal RP. Striatal cholinergic neurotransmission requires VGLUT3. *The Journal of neuroscience : the official journal of the Society for Neuroscience* 2014; **34**(26): 8772-8777.
46. Kravitz AV, Tye LD, Kreitzer AC. Distinct roles for direct and indirect pathway striatal neurons in reinforcement. *Nature neuroscience* 2012; **15**(6): 816-818.

47. Berridge KC. The debate over dopamine's role in reward: the case for incentive salience. *Psychopharmacology* 2007; **191**(3): 391-431.
48. Berridge KC, Robinson TE, Aldridge JW. Dissecting components of reward: 'liking', 'wanting', and learning. *Curr Opin Pharmacol* 2009; **9**(1): 65-73.
49. Kalivas PW, Volkow N, Seamans J. Unmanageable motivation in addiction: a pathology in prefrontal-accumbens glutamate transmission. *Neuron* 2005; **45**(5): 647-650.
50. Wagner FA, Anthony JC. From first drug use to drug dependence; developmental periods of risk for dependence upon marijuana, cocaine, and alcohol. *Neuropsychopharmacology : official publication of the American College of Neuropsychopharmacology* 2002; **26**(4): 479-488.

FIGURE LEGENDS

Figure 1 Enhanced rewarding properties of cocaine in VGLUT3^{-/-} mice. (a) Repeated cocaine injections produced a progressive increase in locomotor sensitization (repeated-measures three-way ANOVA, $F_{(8,156)}=18.39$, $p<0.001$). (b) Cumulative locomotion (30 min) following cocaine injection on the first day (day 4) versus challenge day (day 13). [WT (n=6); VGLUT3^{-/-} (n=6); two-way ANOVA, $F_{(1,18)}=9.52$, $p=0.006$]. (c) VGLUT3^{-/-} mice established conditioned place preference when receiving a dose of 2.5 mg/kg cocaine (n=10-11), whereas a dose of 5 mg/kg elicited preference in both genotypes [(n=7), two-way ANOVA, $F_{(2,47)}=6.419$, $p=0.003$, Bonferroni post-test]. (d) Levels of active nose-poking were significantly higher in VGLUT3^{-/-} mice (n=13) than in WT mice (n=14) during the acquisition (FR1, FR3) of self-administration (three-way ANOVA, $F_{(1,25)}=14.97$; $p<0.01$). Both genotypes showed similar extinction (three-way ANOVA, $F_{(1,24)}=0.08$, $p>0.05$). (e) Number of active nose-pokes during FR1, FR3 and extinction (f) Progressive ratio of cocaine self-administration. VGLUT3^{-/-} mice were more motivated to seek cocaine than WT mice (one-way ANOVA, $F_{(1,25)}=6.78$; $p<0.05$). (g) Cue-induced reinstatement test. VGLUT3^{-/-} mice displayed a higher rate of relapse than WT mice (three-way ANOVA, $F_{(1,25)}=12.43$, $p<0.01$). Newman-Keuls post-test. * $p<0.05$, ** $p<0.01$, *** $p<0.001$. All data are mean±SEM. (Statistical analyses in Supplementary Table S1 and S2.)

Figure 2 Dopamine release is enhanced in the NAc of VGLUT3^{-/-} mice. (a) DA release induced by the first KCl injection (K1) in the NAc of WT (n=14), VGLUT3^{-/-} (n=16, two-way ANOVA, $F_{(1,95)}=25.6$ $p<0.001$) and VACHT^{D2-Cre-flox/flox} (n=11, two-way ANOVA, $F_{(1,73)}=23.8$, $p<0.001$) mice measured by *in vivo* chronoamperometry. (b, c) Accommodation of DA efflux in the NAc of WT, VACHT^{D2-Cre-flox/flox} and VGLUT3^{-/-} mice after 4 consecutive KCl ejections (K1 to K4). (b) Bar plots indicate the maximum of DA release and (c) the T80 induced by consecutive

KCl stimulation. Two-way ANOVA genotype effect ($^{##}p<0.01$, $^{###}p<0.001$), post-hoc Mann-Whitney analysis ($*p<0.05$, $**p<0.01$, $***p<0.001$: red asterisks WT vs. VGLUT3^{-/-}, blue asterisks WT vs. VACHT^{D2-Cre-flox/flox}). (d, e) Effects of the broad-spectrum mGLUR antagonist LY341495 (100 μ M) on K⁺-induced DA efflux in the NAc of WT mice and VGLUT3^{-/-} mice. Black and red hatched areas indicate the release of K⁺-induced DA efflux in WT mice and VGLUT3^{-/-} mice, respectively, as shown in (a). (e) Bar plots indicate the maximum of DA release and the T80 of the DA response induced by KCl in the presence or absence of LY341495 in WT mice and VGLUT3^{-/-} mice. Mann-Whitney. Mann-Whitney analysis ($*p<0.05$, $**p<0.01$, $***p<0.001$). (Statistics in Supplementary Table S3.)

Figure 3 DRD1 signaling cascade, spine density and synaptic transmission in MSNs of VGLUT3^{-/-} mice. Quantification of (a) [¹²⁵I]iodosulpride (DRD2) and (b) [³H]SCH23390 (DRD1). The number of DRD1 binding sites increased in the NAc of VGLUT3^{-/-} mice (n=5; Mann Whitney, $p=0.0317$). (c) Cocaine administered at a dose of 2.5 mg/kg but not 10 mg/kg resulted in a higher number of P-ERK positive cells in the NAc of VGLUT3^{-/-} mice than in the NAc of WT mice (n=5; two-way ANOVA, $F_{(2,22)}=30.22$, $p<0.0001$). (d) VGLUT3^{-/-} mice had a higher density of MSN dendritic spines than WT mice (n=11-14; two-way ANOVA, $F_{(1,33)}=6.443$, $p<0.001$). Chronic cocaine administration increased spine density only in WT mice (two-way ANOVA, $F_{(1,33)}=14.21$, $p=0.006$). (e-f) VGLUT1 and VGLUT2 densities are unchanged in VGLUT3^{-/-} mice. (g) EPSCs recorded at -60 and +40 mV from WT and VGLUT3^{-/-} mice. AMPA/NMDA ratios were higher in slices from mutant mice (n=6-8; WT, 2.3 ± 0.3 ; VGLUT3^{-/-}, 3.5 ± 0.4 $t_{12}=2.6$, $p<0.05$). (h) mEPSCs recorded in WT and VGLUT3^{-/-} mice. (i) mEPSC frequency (n=10; WT, 0.82 ± 0.1 Hz; VGLUT3^{-/-}, 4.1 ± 1 Hz; $t_{18}=2.9$, $p<0.01$) and (j) amplitude (n=10; WT, 23.8 ± 1.1 pA; VGLUT3^{-/-}, 23.2 ± 0.6 pA; $t_{18}=0.4$, $p>0.05$). (k) Paired-pulse ratio (n=7-9; WT, 1.1 ± 0.1 ; VGLUT3^{-/-}, 1.2 ± 0.05 ; $t_{14}=0.3$, $p>0.05$). $*p<0.05$, $**p<0.01$, $***p<0.001$. All data are mean \pm SEM.

Figure 4 VGLUT3 deletion mediates structural and functional adaptations onto DRD1

MSNs. (a) The number of DRD1a-positive neurons was not different in the NAc or in the dorsal striata of WT:DRD1a-EGFP⁺ (n=11) and VGLUT3^{-/-}:DRD1a-EGFP⁺ mice (n=17, two-way ANOVA, $F_{(1,47)}=0.0823$, $p=0.775$). (b) VGLUT3^{-/-} had a higher spine number in DRD1a-EGFP positive cells (EGFP⁺) (WT n=15, VGLUT3^{-/-} n=19, two-way ANOVA, $F_{(1,64)}=15.10$, $p<0.001$) but not in DRD1-negative MSN (DRD1a-EGFP⁻, labeled with Dil; WT n=13, VGLUT3^{-/-} n=19). (c) DIC and fluorescence channel image of a D1-EGFP⁺ patched neuron. (d) Sample traces of EPSCs recorded at -60 and +40 mV in WT and VGLUT3^{-/-} Drd1a-EGFP positive and negative. (e) Bar graph and scatter plot for AMPA/NMDA ratios recorded in WT and VGLUT3^{-/-} Drd1a-EGFP positive and negative (n=8-10; WT - Drd1a-EGFP⁺, 2.6 ± 0.4 ; VGLUT3^{-/-} - Drd1a-EGFP⁺, 3.9 ± 0.4 ; $t_{16}=2.1$, $p<0.05$; WT - Drd1a-EGFP⁻, 2.2 ± 0.3 ; VGLUT3^{-/-} - Drd1a-EGFP⁻, 2.1 ± 0.1 ; $t_{15}=0.3$, $p>0.05$; * $p<0.05$, ** $p<0.01$, *** $p<0.001$. All data are mean \pm SEM.

Figure 5 VGLUT3 mutations in humans with severe drug abuse. Seven mutations were identified in patients with severe addiction. The topological structure of VGLUT3 is depicted in the synaptic vesicle membrane based on protein structure described under accession Q8NDX2. Amino acids affected by the mutations are shown in red. The chromatogram corresponding to the DNA sequence observed in patients as well as the VGLUT3 protein alignment in six vertebrates is shown for each variation predicting an amino acid change.

Figure 6 Dual regulation of DA efflux by ACh and glutamate released by TANS in the NAc.

TANs express VAcHT and VGLUT3 and therefore co-release ACh and glutamate. These 2 co-transmitters exert opposing effects on DA release. In WT mice, (a) DA efflux is stimulated by

ACh (through nAChRs) and inhibited by VGLUT3-dependent glutamate (through mGLURs most likely located on DA terminals). In VGLUT3^{-/-} mice (b), the mGLUR-driven inhibition is lost and therefore DA efflux is markedly enhanced. Consequently the DRD1 signaling cascade is over-activated, and dendritic spine density (without modification of the number of excitatory terminals) and cortico-striatal glutamatergic activity are increased, leading to augmented sensitivity to the rewarding properties of cocaine.

Table 1. Summary of the variations identified in the human *SLC17A8* coding sequence

| Populations | Total number of subjects | Number of missense variations (% of alleles) | Number of subjects carrying missense variations (% of alleles) | Number of synonymous variations (% of alleles) | Number of subjects carrying synonymous variations (% of alleles) |
|---------------------|--------------------------------|---|---|---|---|
| French addicts | 230 | 7 (1.5) | 12 (2.6) | 2 (0.4) | 4 (0.9) |
| Swiss addicts | 265 | 4 (0.8) | 4 (0.8) | 2 (0.4) | 5 (0.9) |
| French controls | 213 | 1 (0.2) | 1 (0.2) | 1 (0.2) | 1 (0.2) |
| 1000 Genome Project | 1092 | 8 (0.4) | 26 (1.2) | 10 (0.5) | 145 (6.6) |

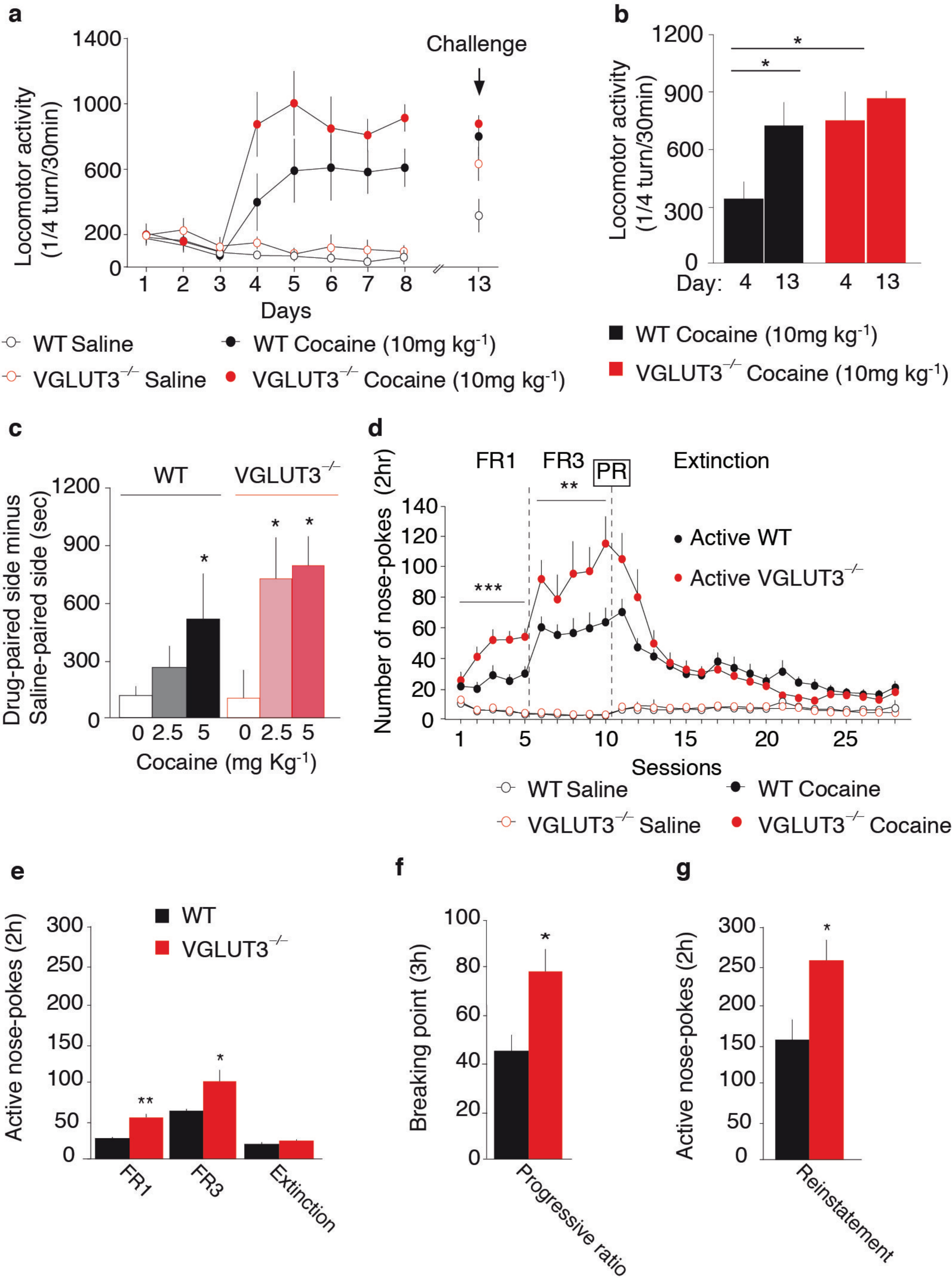


Figure 1 Sakae et al.

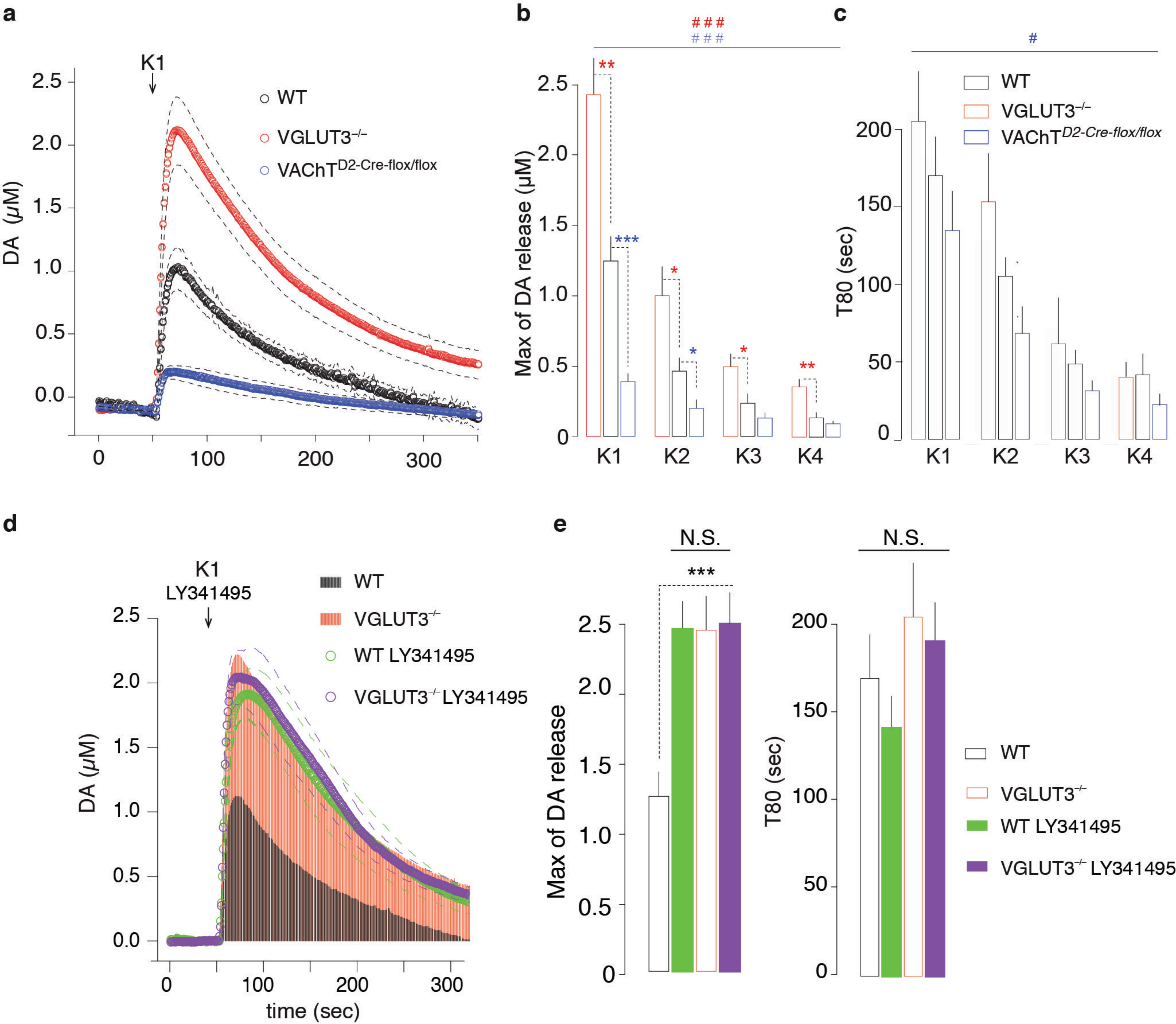


Figure 2 Sakae et al.

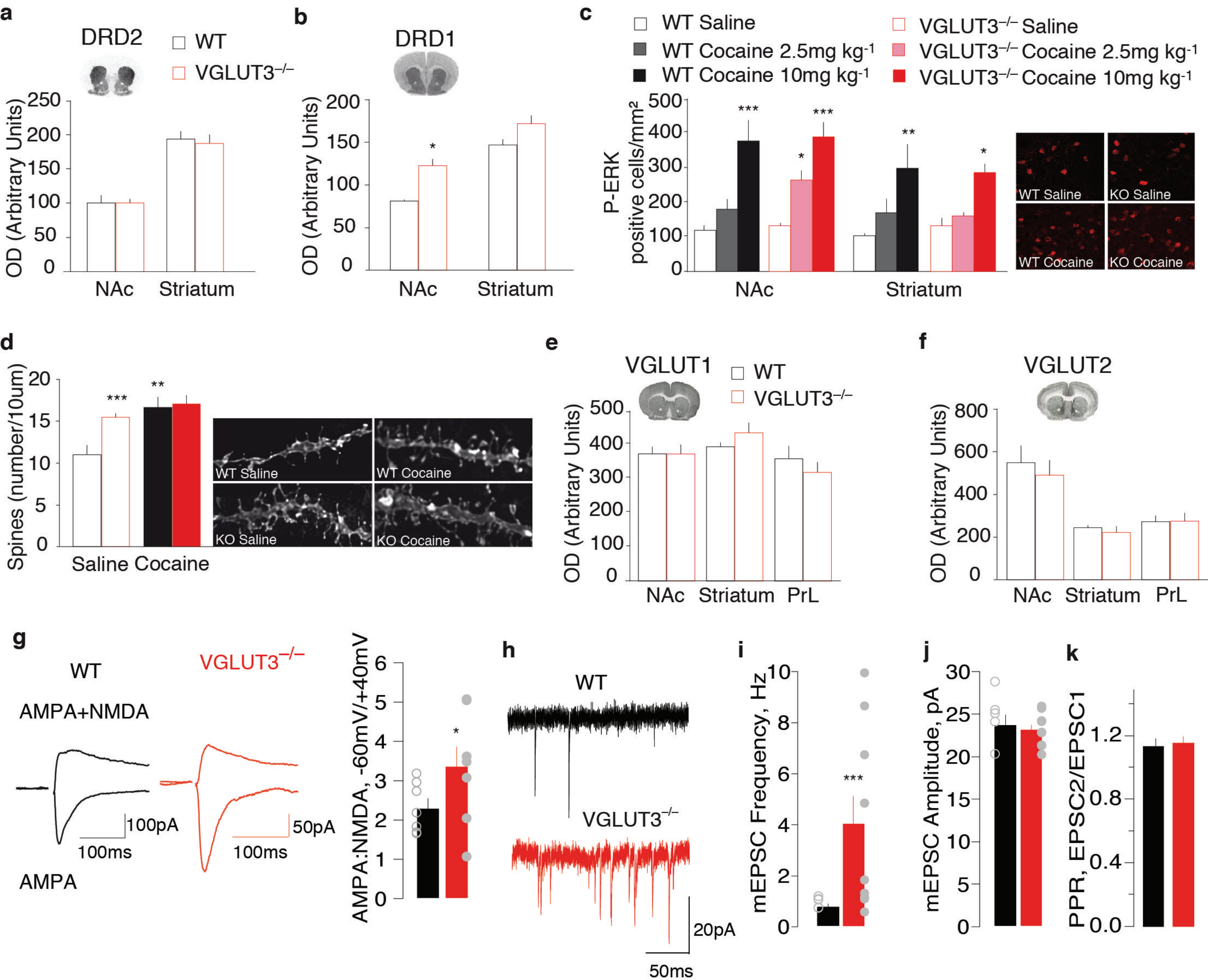


Figure 3 Sakae et al.

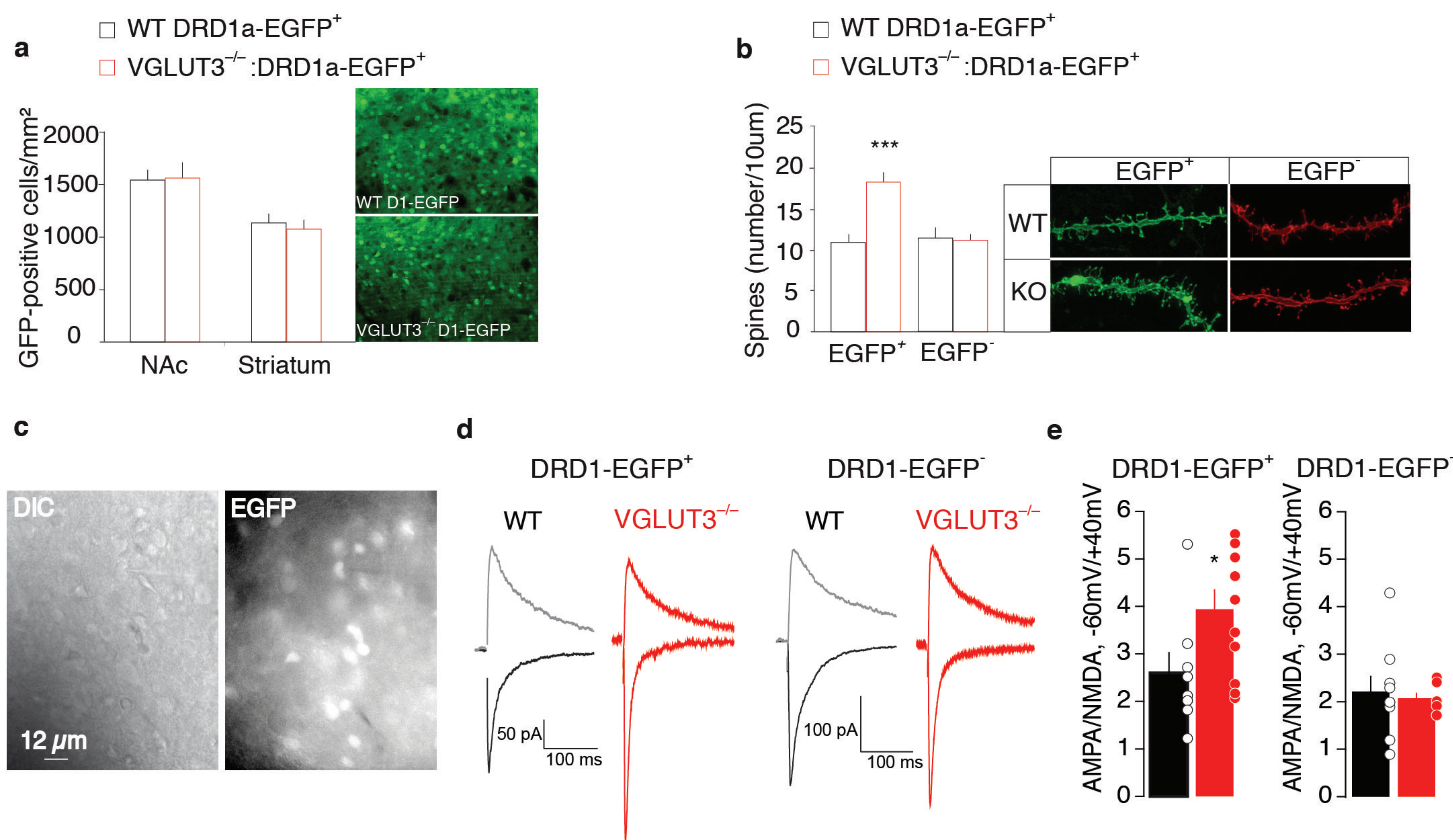
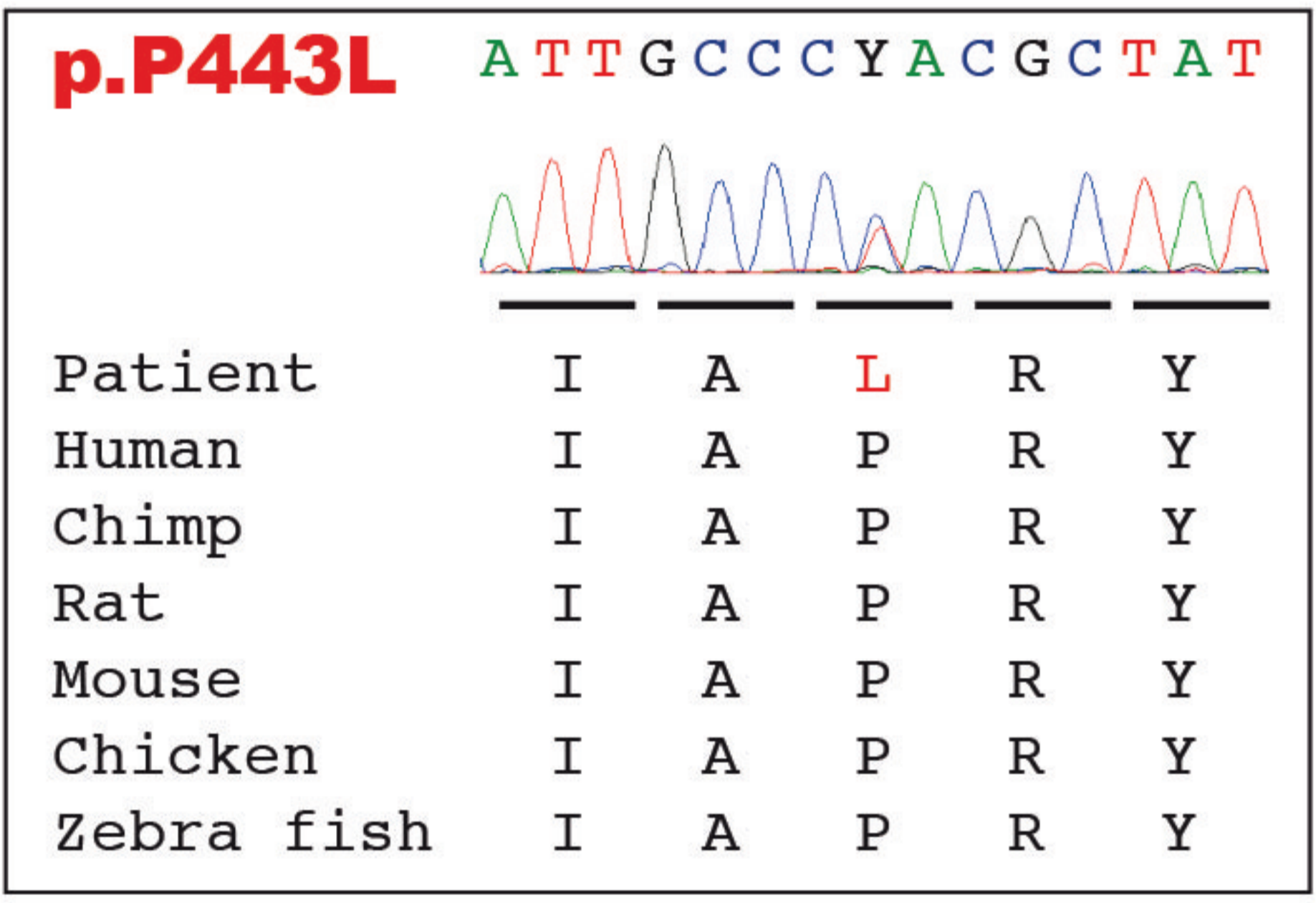
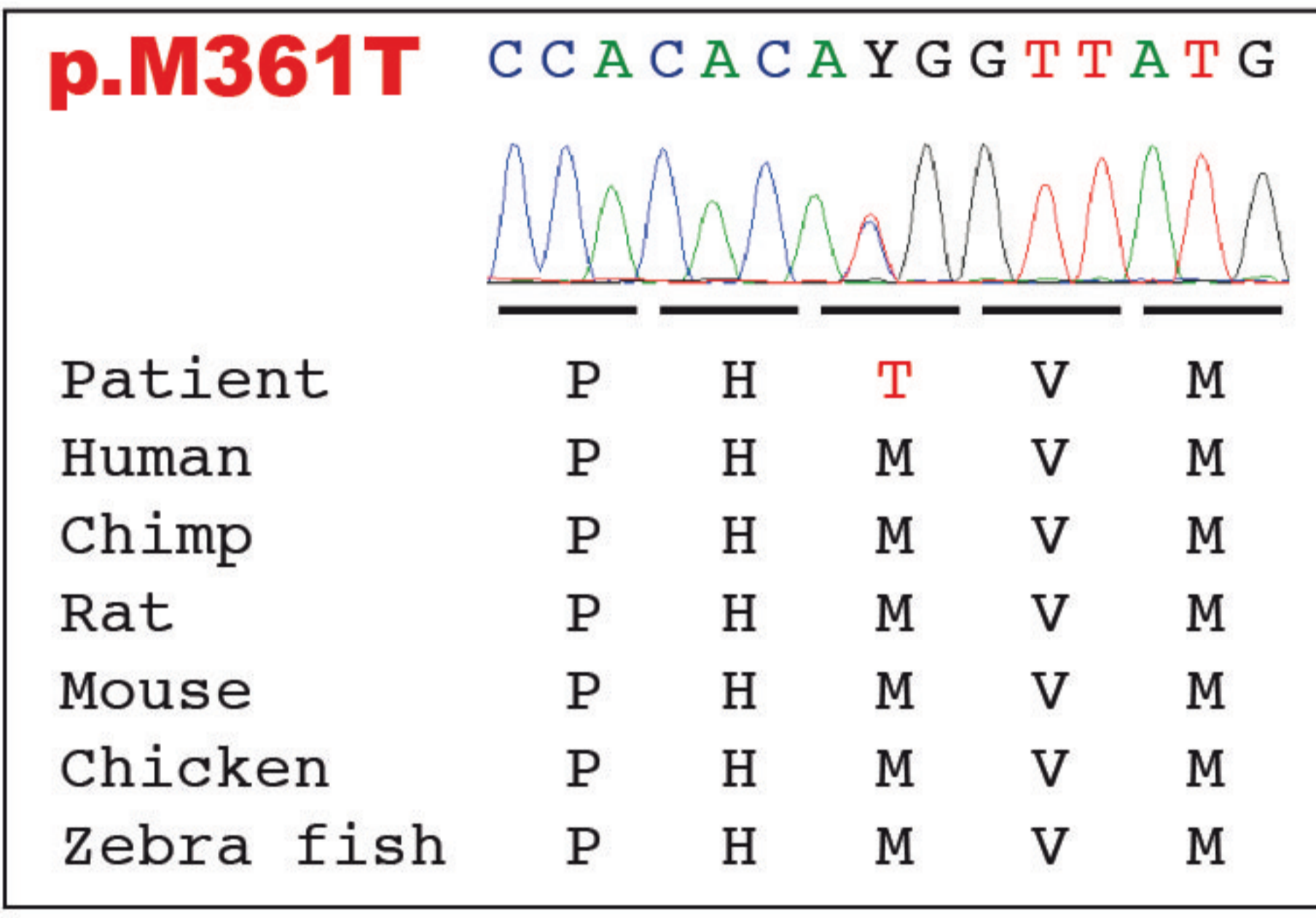
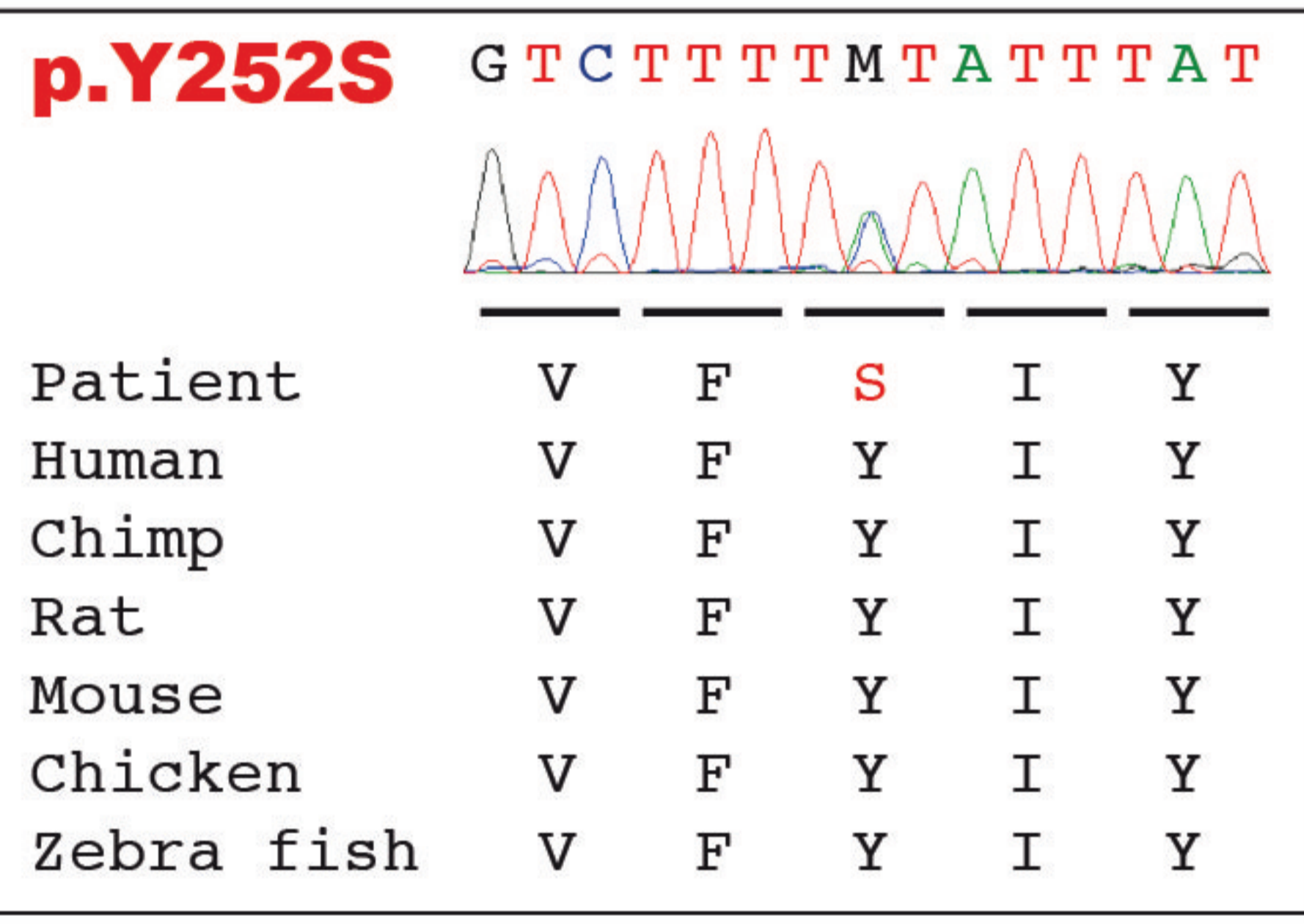
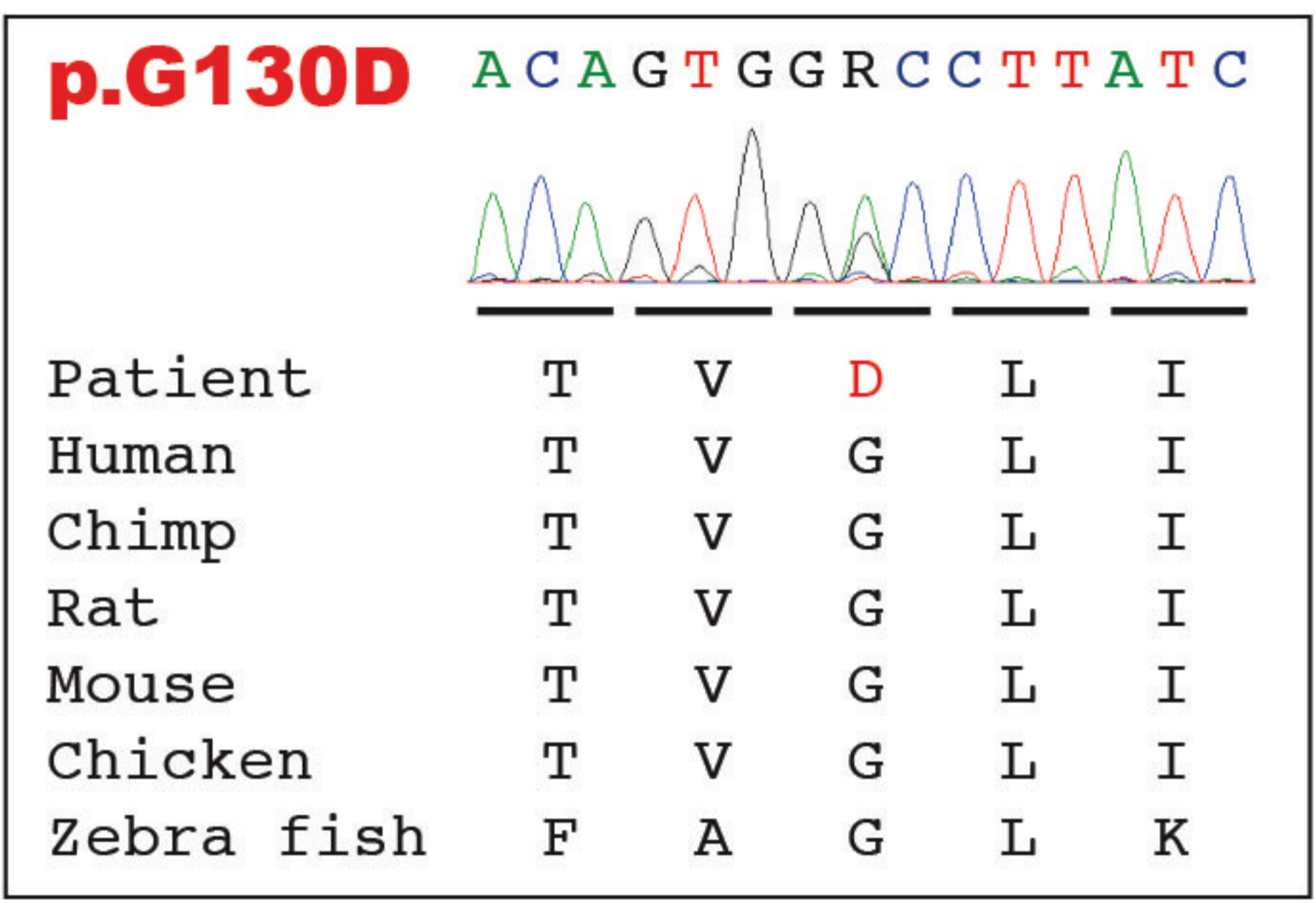
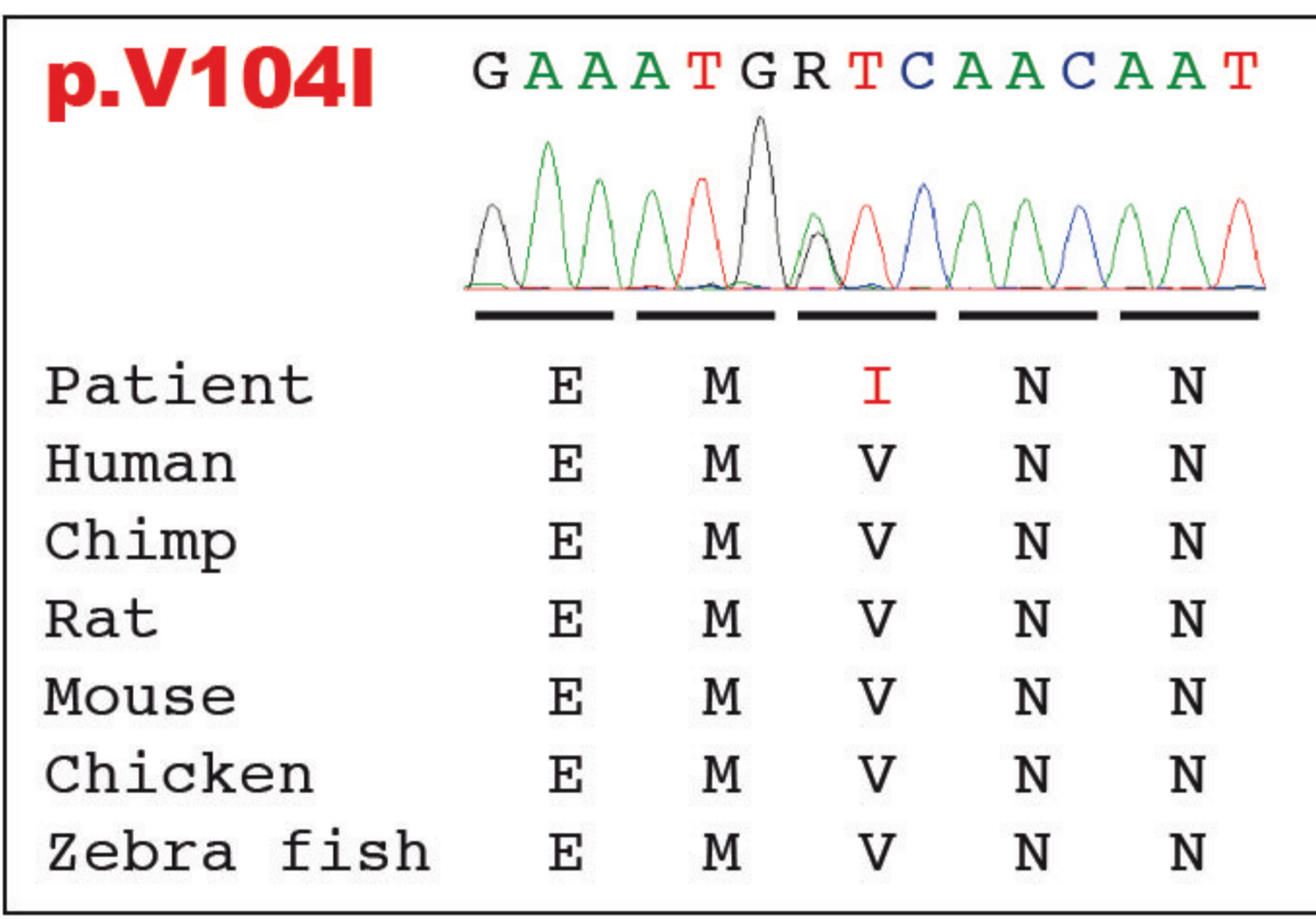
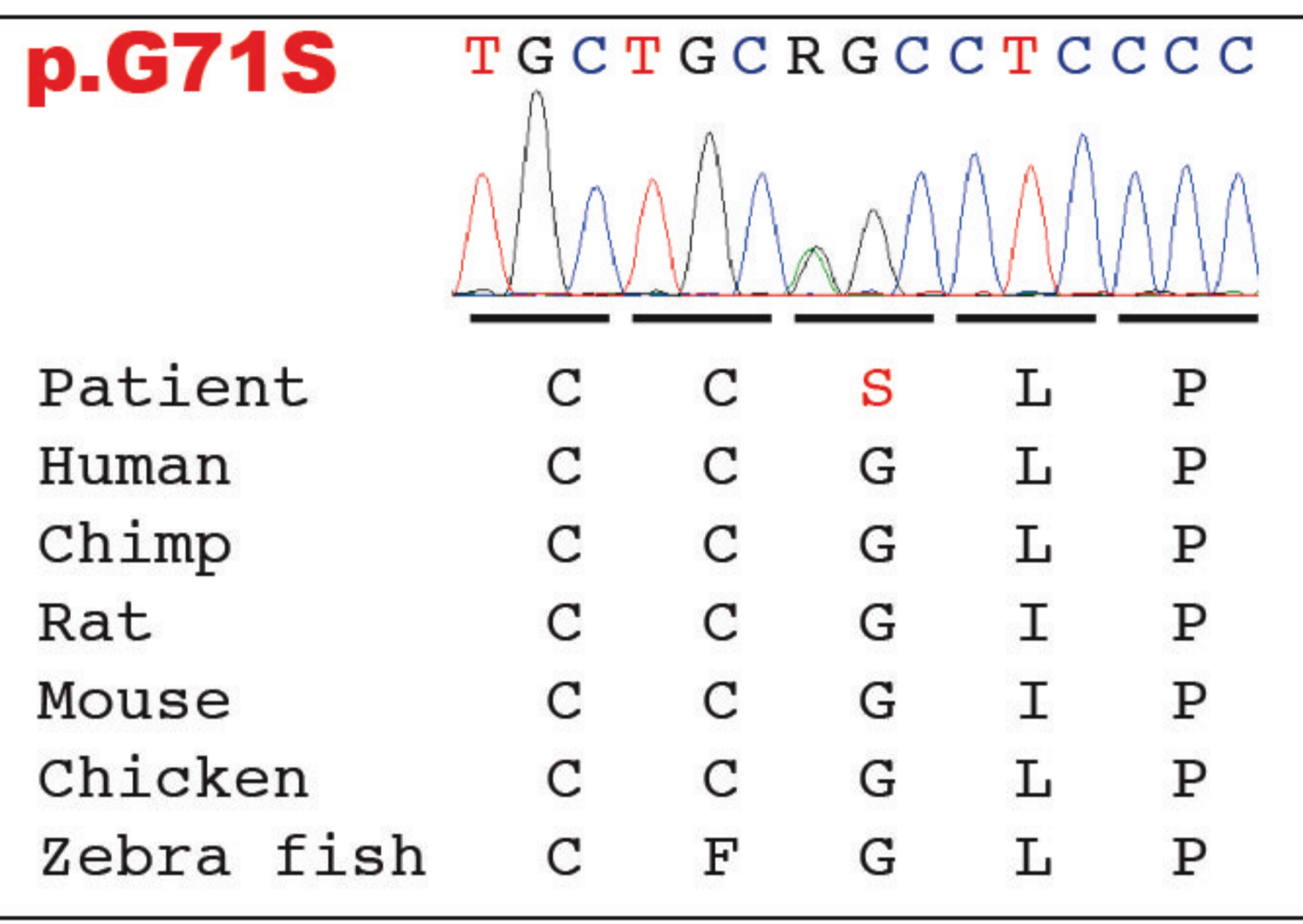
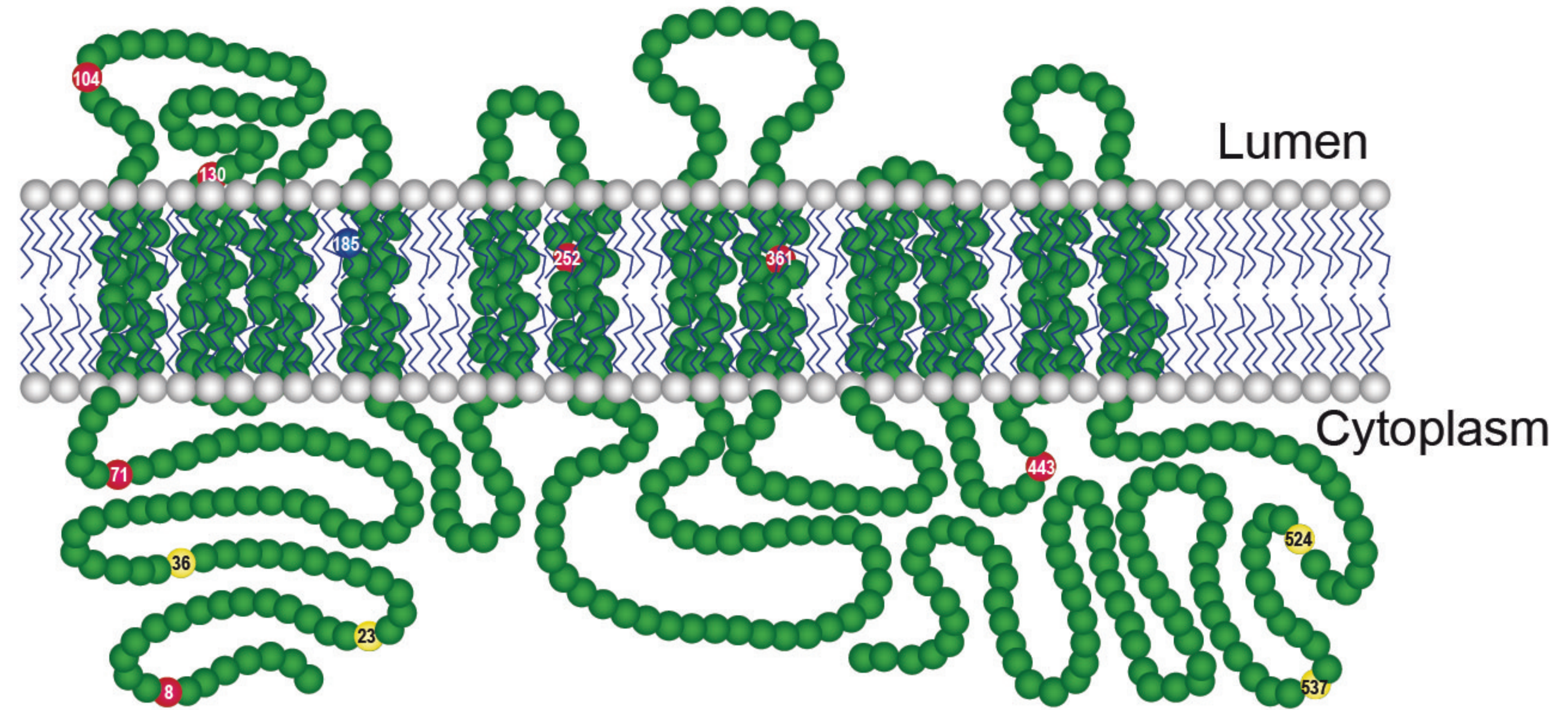
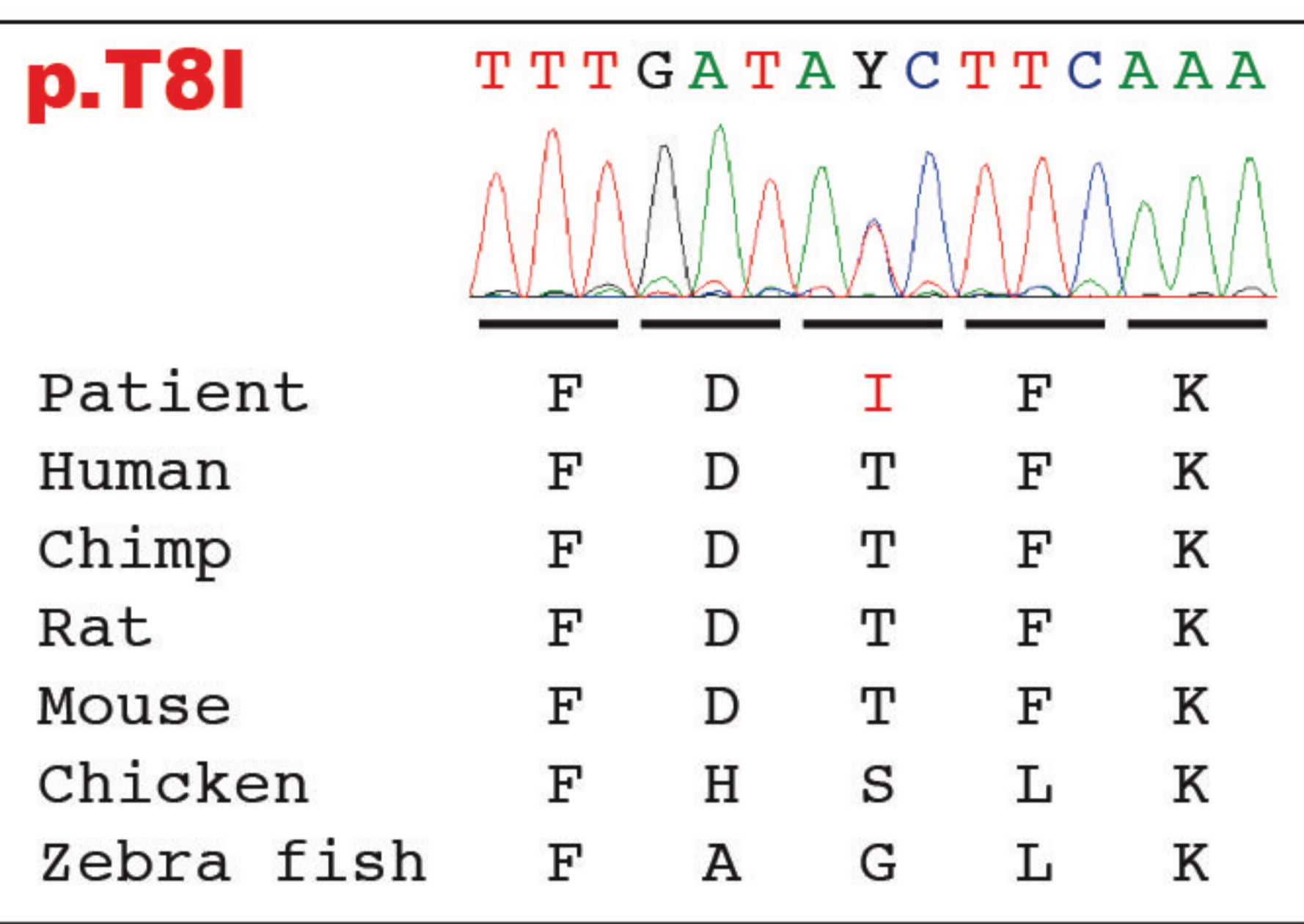
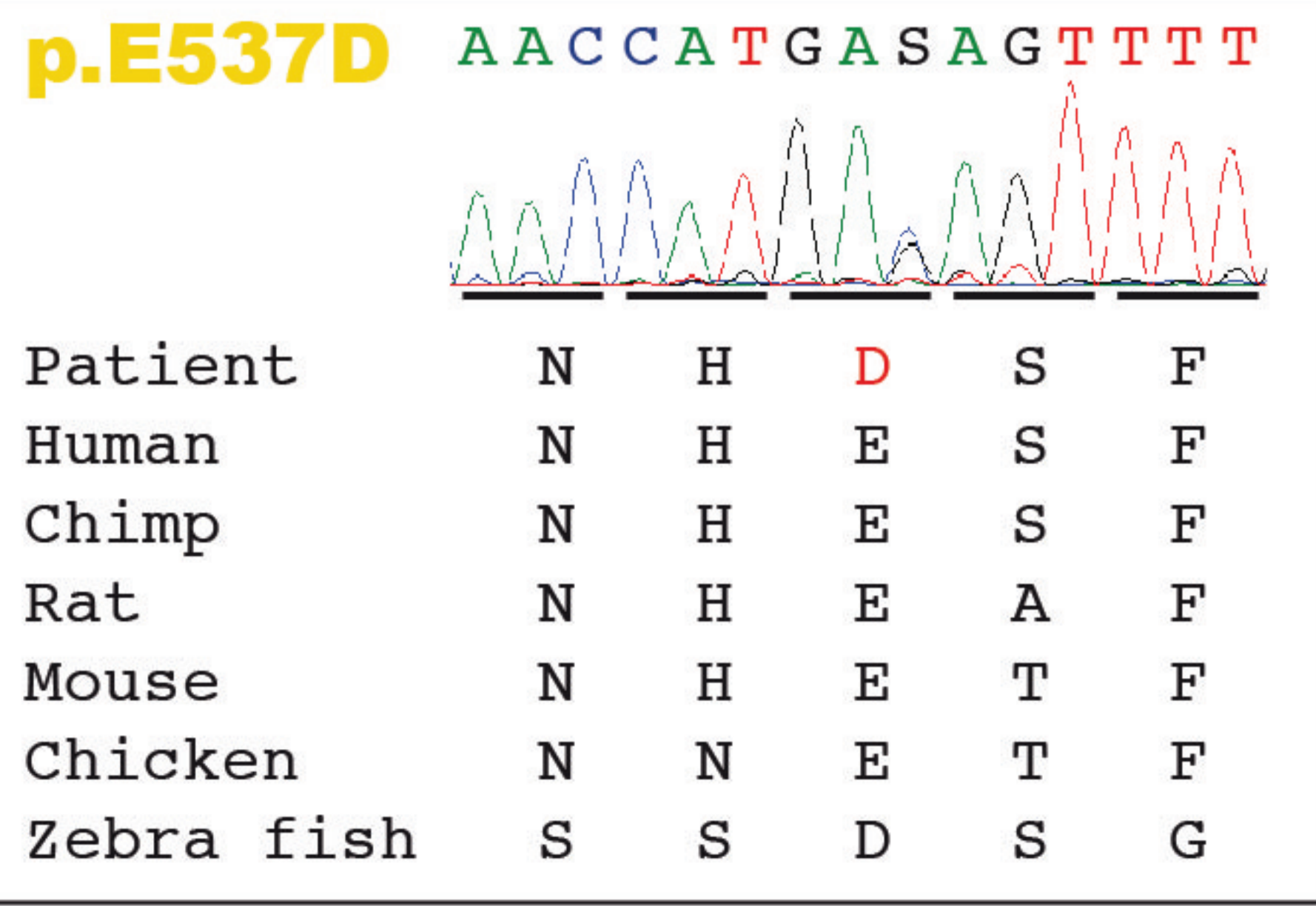
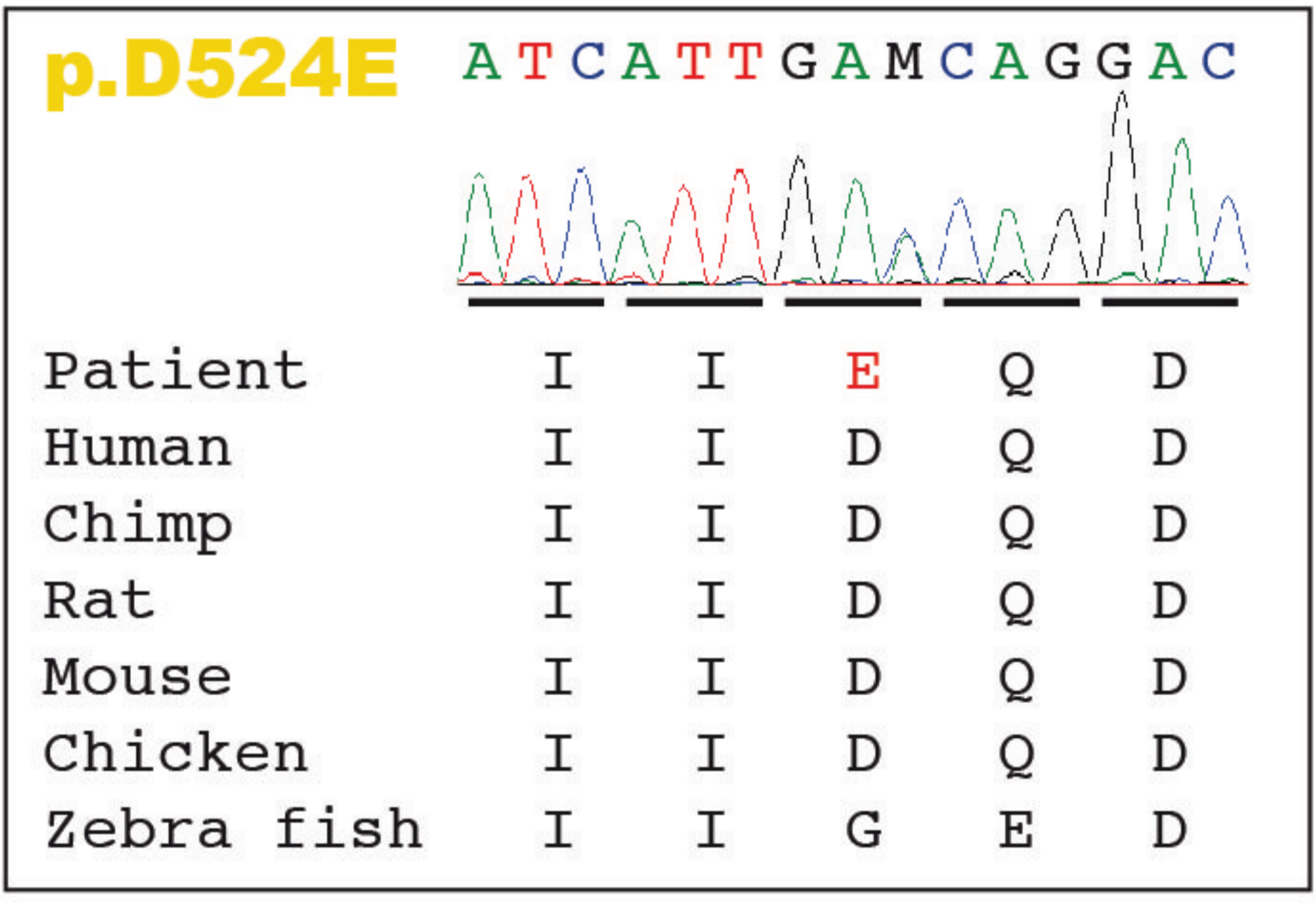
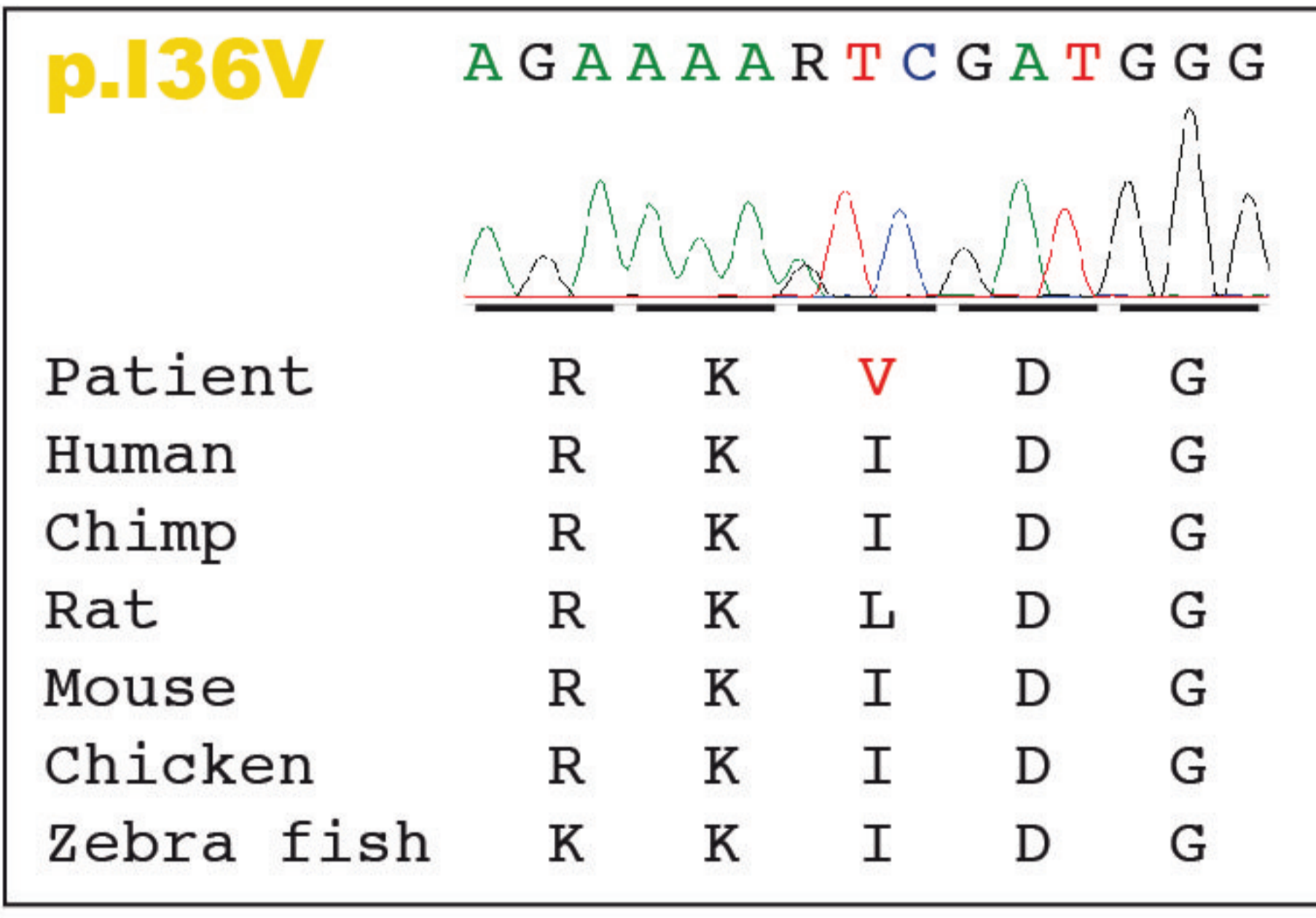
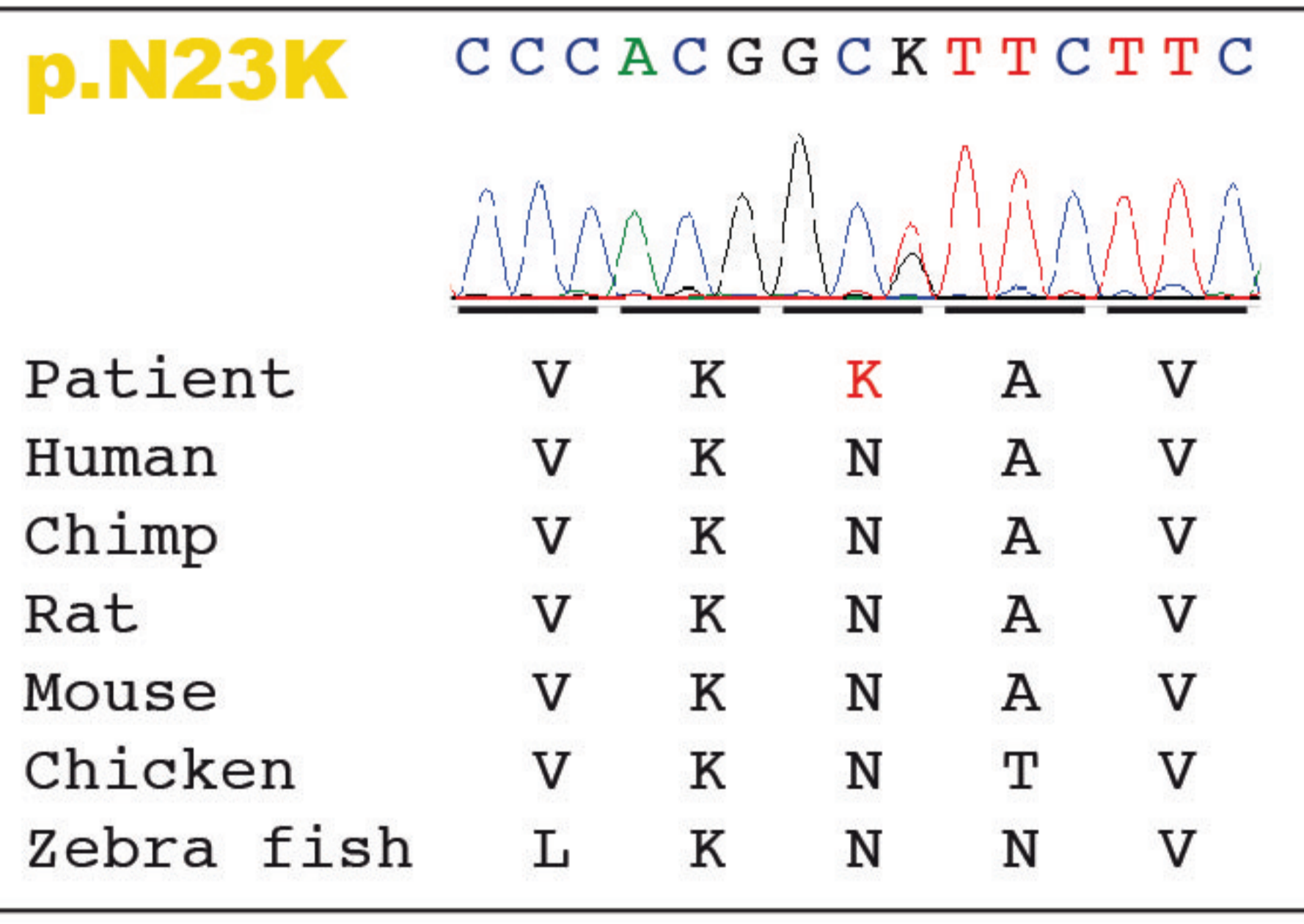


Figure 4 Sakae et al.

French addicts



Swiss addicts



French controls

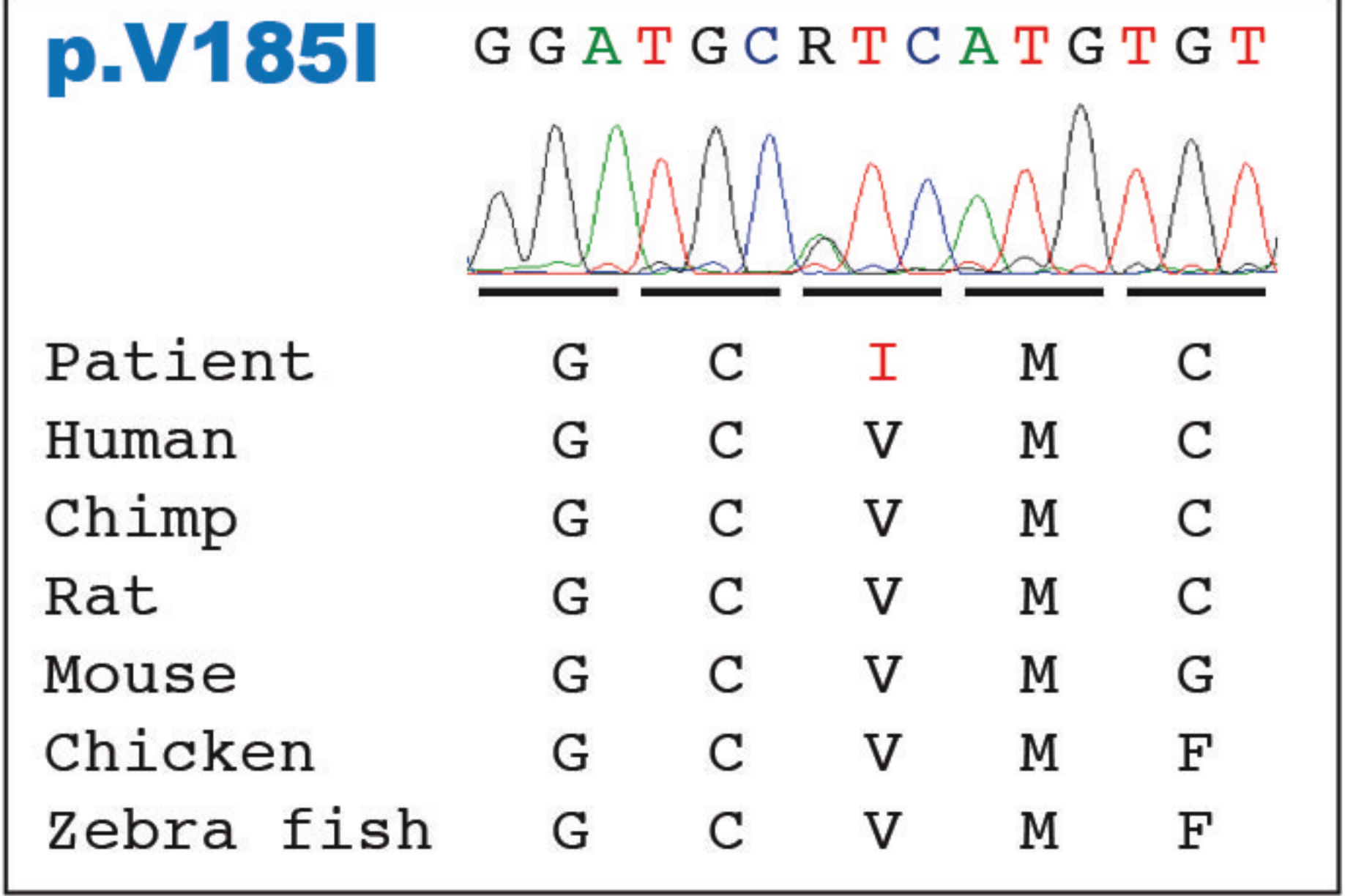
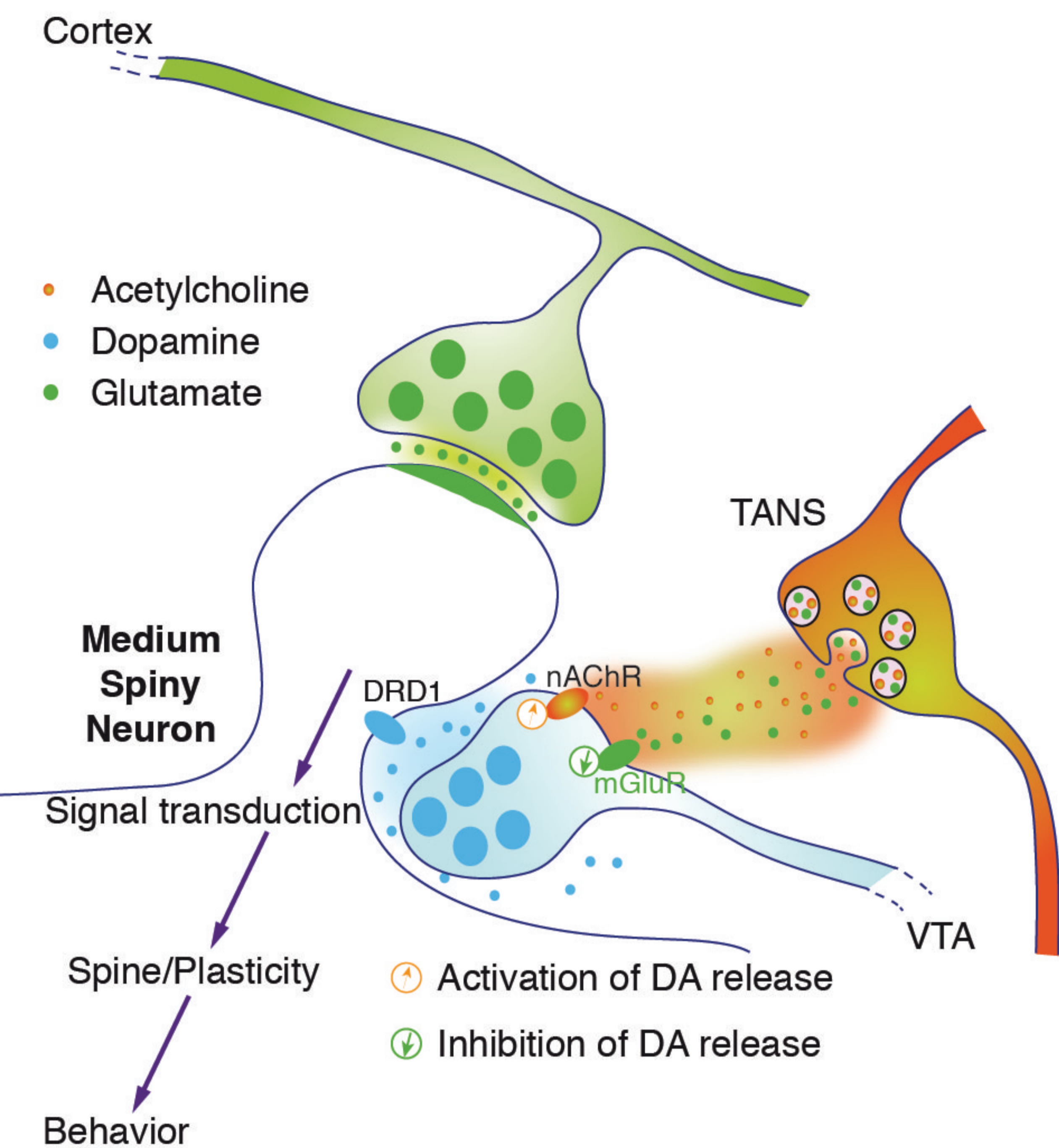


Figure 5 Sakae et al.

a VGLUT3^{+/+} mice



b VGLUT3^{-/-} mice

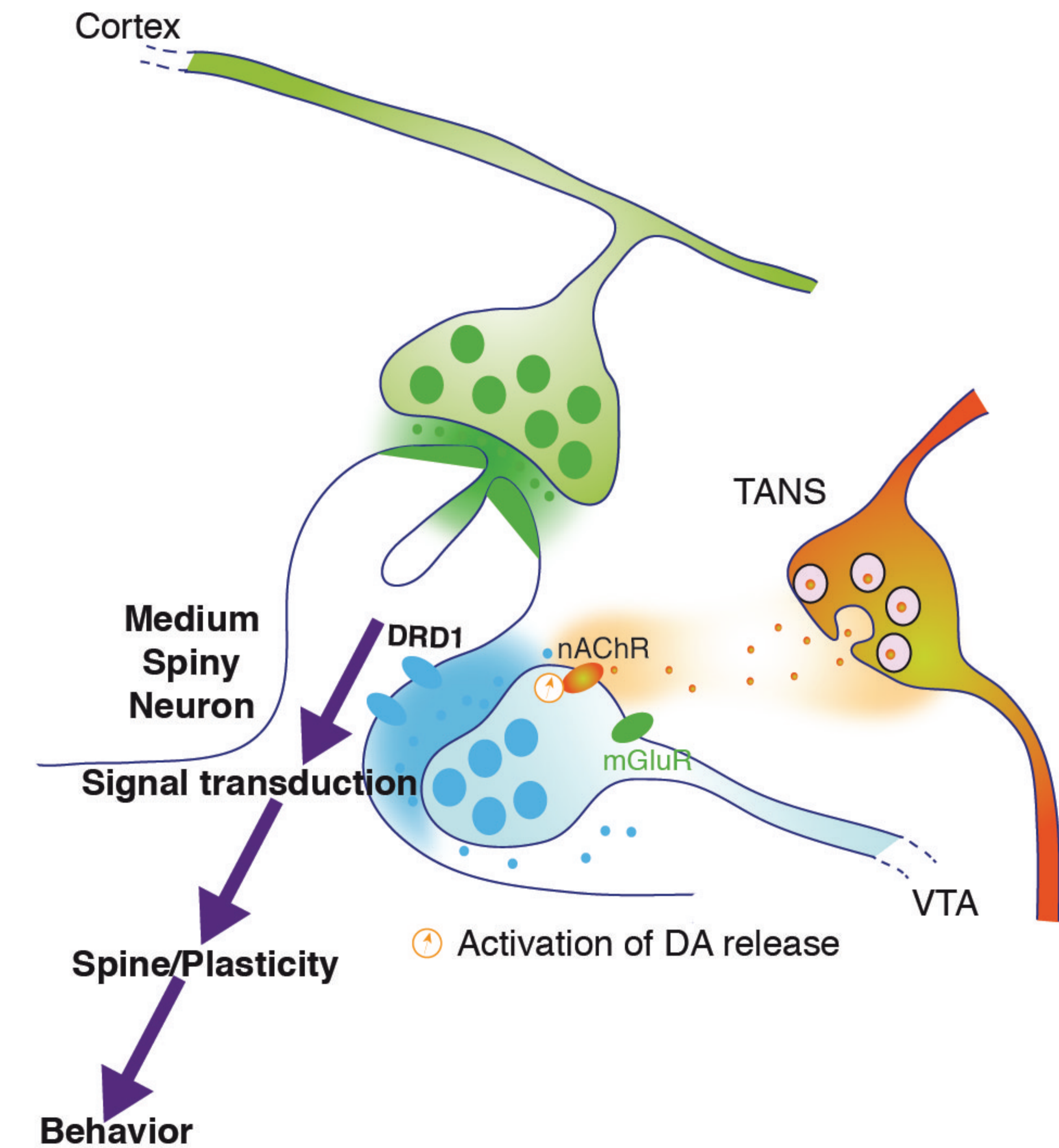


Figure 6 Sakae et al.